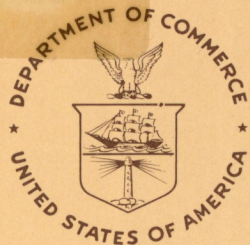


QC  
807.5  
U66  
no.396

NOAA Technical Report ERL 396-ARL 5



# The Mauna Loa Four Wavelength Nephelometer: Instrument Details and Three Years of Observations

Barry A. Bodhaine

April 1978

**U.S. DEPARTMENT OF COMMERCE**  
National Oceanic and Atmospheric Administration  
Environmental Research Laboratories



QC  
807.5  
1166  
ml. 396

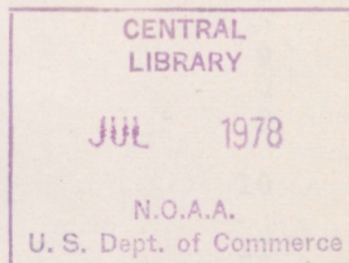


# The Mauna Loa Four Wavelength Nephelometer: Instrument Details and Three Years of Observations

Barry A. Bodhaine

Air Resources Laboratories/GMCC  
Boulder, Colorado

April 1978



## U. S. DEPARTMENT OF COMMERCE

Juanita M. Kreps, Secretary

National Oceanic and Atmospheric Administration

Richard A. Frank, Administrator

Environmental Research Laboratories

Wilmot Hess, Director



# NOTICE

Mention of a commercial company or product does not constitute an endorsement by NOAA Environmental Research Laboratories. Use for publicity or advertising purposes of information from this publication concerning proprietary products or the tests of such products is not authorized.



## CONTENTS

Abstract	1
1. Introduction	1
2. The Instrument and Its Use	3
2.1 Theory of Calibration	4
2.2 Checking Linearity	5
2.3 Resetting Sample Time	5
3. Nephelometer Data	6
3.1 Data in Appendix A	7
3.2 Data in Appendix B	8
3.3 Data in Appendix C	9
4. Summary	9
5. Acknowledgments	9
6. References	10
Appendix A	11
Appendix B	31
Appendix C	39



THE MAUNA LOA FOUR WAVELENGTH NEPHELOMETER:  
INSTRUMENT DETAILS AND THREE YEARS OF OBSERVATIONS

Barry A. Bodhaine

Abstract. Three years of high quality total light scattering data from a four-wavelength integrating nephelometer have been acquired at Mauna Loa Observatory as part of the Geophysical Monitoring for Climate Change (GMCC) program. These data may be representative of the upper troposphere under certain weather conditions and may therefore be used to deduce background global aerosol properties and their possible effect on climate. A light scattering value of about  $b_{sp}(550 \text{ nm}) = 10^{-7} \text{ m}^{-1}$  appears to be a good estimate of the light scattering of aerosols during the cleanest background conditions at Mauna Loa Observatory.

1. INTRODUCTION

This report presents total light scattering data taken with a four wavelength nephelometer at Mauna Loa Observatory from January 1974 to December 1976. A brief description of the principles and operation of the instrument is included to aid the potential user in data interpretation. The user may wish to use this report for a first look at the data and to identify specific events to be examined more closely. A complete set of hourly means of four wavelengths of light scattering data, along with meteorological data, may be obtained from NOAA-ARL-GMCC, Boulder, Colorado 80302.

The nephelometer approach to the measurement of the integrated light scattering of air was first attempted by Beuttell and Brewer (1949) and later refined by Crosby and Koerber (1963) who used a photomultiplier tube as the sensing element. Mechanical and electrical design were improved by Ahlquist and Charlson (1967), and the sensitivity of the instrument was improved to the point where the Rayleigh or molecular scattering coefficients of various gases could be measured. In comparisons between the light scattering coefficient of ambient air and total suspended particulate mass made by Charlson et al. (1967), the



simple linear relationship  $M = 0.38 b_{\text{scat}}$ , where  $M$  is mass in  $\text{g m}^{-3}$  and  $b_{\text{scat}}$  is in  $\text{m}^{-1}$ , was found to hold true approximately for a variety of natural and anthropogenic aerosol sources. The standard integrating broadband nephelometer manufactured by Meteorology Research Inc. (Charlson et al., 1969) has gained wide use for the measurement of visual range and air quality, and has been increased in sensitivity by using photon counting techniques in place of the old flashlamp-analog signal technique.

Because light scattering is responsible for many chromatic atmospheric effects (blue sky, colorful sunsets, etc.), the wavelength dependence of light scattering by air molecules and aerosol particles has received much attention since the classical works of Rayleigh (1871), Mie (1908), and Angstrom (1929). Angstrom concluded that the wavelength dependence of aerosol scattering could be described by  $b_{\text{scat}} \approx \lambda^{-\alpha}$  in a manner similar to that used for Rayleigh scatter by gases, where  $b_{\text{scat}}$  is the extinction coefficient due to scatter,  $\lambda$  is the wavelength, and  $\alpha$  is the Angstrom exponent. Typical values of  $\alpha$  for aerosol scatter are about 1.5, and pure Rayleigh or molecular scatter gives  $\alpha = 4$ .

A simple relationship between the aerosol size distribution and the Angstrom exponent for aerosol scatter has been developed and is summarized by Butcher and Charlson (1972). Whitby (1975) has shown that particle size distributions are probably best described by a multi-modal log normal curve fit. However, the Junge (1963) power law model for the size distribution of aerosols,

$$\frac{dN}{d \log r} = Cr^{-\beta},$$

where  $dN$  is the number of particles in the radius increment  $d \log r$ ,  $\beta$  is the slope of the size distribution, and  $C$  is a constant, is a good approximation over a limited size range. The simple relationship  $\alpha = \beta - 2$  makes it possible to obtain aerosol size distribution information by measuring the Angstrom exponent, i.e., by measuring light scattering at several different wavelengths. An instrument to measure light scattering as a function of wavelength was developed by Ahlquist and Charlson (1969) and used extensively in field experiments (Charlson, 1972) to measure the Los Angeles smog aerosol.



## 2. THE INSTRUMENT AND ITS USE

The Mauna Loa four-wavelength nephelometer is based on the original Ahlquist and Charlson (1969) design and was manufactured by Meteorology Research, Inc. Preliminary data were reported by Bodhaine and Mendonca (1974). An operational description and calibration procedure is given in detail in the manual supplied with the instrument. Briefly, the nephelometer measures the scattering coefficient of atmospheric gases and particles, and the optical geometry of the instrument provides integration of the scattering over all angles from about  $7^\circ$  to  $170^\circ$ . Scattered light is detected by photon counting techniques, and a rotating filter wheel just in front of the photomultiplier tube allows the measurement of scattering coefficients in four wavelength bands centered at 450, 550, 700, and 850 nm. Digital counting and multiplexing circuitry along with digital-to-analog conversion and logarithmic amplification provide an electrical output proportional to the logarithm of the scattering coefficient at each wavelength. Absolute calibration is provided by the known Rayleigh scattering coefficients of certain gases such as air,  $\text{CO}_2$ , and Freon.

In order to separate the aerosol scattering from the molecular scattering of air and the background

of the instrument, two modes are provided. In the NORMAL mode, the counters count up when a filter is passing light and count down for an equal period when a dark disk is in front of the photomultiplier tube. In addition, an electrical signal simulating molecular scattering of air is subtracted from the output signal. In the AIR CHOP mode, the counters count up on ambient air when a filter is passing light. The instrument is then filled with filtered air and the counters count down for an equal period of time, thus subtracting molecular scatter and instrument background as well. Operation in the NORMAL mode gives better time response and may be used under conditions of fairly high aerosol scatter such as those in urban areas. However, operation in the AIR CHOP mode is necessary in a clean or background location such as Mauna Loa and is capable of measuring aerosol scatter as low as 1% of the molecular scattering of air. Waggoner et al. (1976) have discussed the theory and measurement of the noise level of a four-wavelength nephelometer and find a value of about  $5 \times 10^{-8}$  for a 45-minute averaging time. Furthermore, it has been found that short term fluctuations in photomultiplier dark count are primarily responsible for the instrument noise level.



## 2.1 Theory of Calibration

The nephelometer essentially measures the photon count rate present at the photocathode of a photomultiplier tube, because of the light scattering cross section in the sample volume of the instrument. Mie scattering theory predicts that count rate is a linear function of the scattering cross section, or  $R = C_o b_{sp}$ , where  $R$  is count rate,  $b_{sp}$  is light scatter coefficient, and  $C_o$  is a constant. The nephelometer measures the count rate, takes the logarithm, and presents an output in volts. The output element is a buffer amplifier which incorporates a span and bias adjustment so that

$$V = C_1 \log R + C_2,$$

where  $V$  is output voltage,  $C_1$  is the span, and  $C_2$  is the bias level. We have

$$R = C_o b_{sp}$$

$$\text{or } \log R = \log b_{sp} + \log C_o$$

$$\text{and } V = C_1 \log b_{sp} + (C_1 \log C_o + C_2)$$

$$\text{or } \log b_{sp} = C_3 V + C_4$$

where  $C_3 = 1/C_1$  depends on the span adjustment, and  $C_4 = -(\log C_o + C_2/C_1)$  depends on instrument geometry, span, and bias so that once the span is set it depends only on bias adjustment. Therefore, the relationship between the logarithm of  $b_{sp}$  and the output voltage may be set by two simple adjustments: (1) a volts-per-decade span adjustment

and, (2) a bias adjustment, which together correspond to the point-slope determination of a straight line.

In practice, the slope is set by the volts-per-decade adjustment on the output buffer by presetting the reversible counters with known counts and then adjusting the output to exactly 2 volts per decade. The instrument is then filled with Freon-12, and the bias adjustments (called gain controls on the nephelometer) are set so that Freon scattering coefficients are as shown in Table 1.

TABLE 1. FREON SCATTERING COEFFICIENTS FOR DIFFERENT NEPHELOMETER WAVELENGTHS

Wavelength	Light Scattering	Voltage
450 nm	$2.8 \times 10^{-4} \text{m}^{-1}$	6.8943
550 nm	$1.3 \times 10^{-4} \text{m}^{-1}$	6.2279
700 nm	$4.7 \times 10^{-5} \text{m}^{-1}$	5.3442
850 nm	$2.2 \times 10^{-5} \text{m}^{-1}$	4.6848

These settings define the simple relationship between light scattering coefficient and output voltage:

$$b_{sp} = 10^{\left(\frac{V}{2} - 7\right)}$$

$$\text{or } \log b_{sp} = \frac{V}{2} - 7$$

After the four wavelengths have been calibrated using Freon-12 gas, the instrument is filled with clean air and a calibration object (thin wire with white tip) is introduced into



the sample volume. This object is "white" with high accuracy over the entire visible spectrum and provides a highly stable calibration object for the nephelometer. The light scattering coefficient of this object is "measured" and all channels are trimmed to the 550 nm channel value. This trims the Freon-12 calibration and corrects for the transmission characteristics of the thin film filters used in the instrument.

## 2.2 Checking the Linearity of the Instrument

The instrument is operated over a span of 5 decades, the calibration point is in the upper decade, and most of our data are in the lower 3 decades. It is therefore desirable to check the linearity of the D to A converter, log amplifier, and other output circuitry. The instrument calibration for an output of 0 to 10 volts over a 5-decade range is defined by

$$b_{sp} = 10^{\left(\frac{V}{2} - 7\right)}.$$

Therefore, the linearity may be checked by presetting the counters to known counts and measuring the

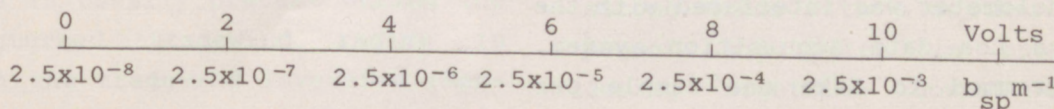
output voltage. The instrument is equipped with the necessary controls so that a linearity check may easily be accomplished over its entire 5-decade range.

## 2.3 Resetting the Sample Time of the Instrument

After the nephelometer is calibrated, it has a 0-10 volt output at 2 volts per decade with a lower limit of  $b_{sp} = 10^{-7} \text{ m}^{-1}$ . Since this is not sufficiently sensitive for monitoring at Mauna Loa, the sample time of the instrument is increased by a factor of 4, which effectively increases the instrument sensitivity by a factor of 4. The new relationship between light scattering and output voltage is

$$b_{sp} = 0.25 \times 10^{\left(\frac{V}{2} - 7\right)}.$$

Because of the logarithmic output, the scale is simply shifted so that the lower limit is  $b_{sp} = 2.5 \times 10^{-8} \text{ m}^{-1}$ , and the span of 5 decades, at 2 volts per decade, is retained. For purposes of data reduction, therefore, the following scale is used:





### 3. NEPHELOMETER DATA

The Mauna Loa four-wavelength nephelometer has operated continuously since January 24, 1974. Reliability has been very good, and only about 5% of the data were lost during the first 3 years. Some of the downtime was caused by the multipoint recorder rather than the nephelometer itself. Data were continuously recorded on a 12-channel Leeds and Northrup multipoint strip chart recorder operated at a chart speed of 2 inches per hour. The chart is 10 inches wide and spans 5 decades of light scattering ( $b_{sp} = 2.5 \times 10^{-8} \text{ m}^{-1}$  to  $2.5 \times 10^{-3} \text{ m}^{-1}$ ). The output of the nephelometer has an electrical time constant of 45 minutes, which produces a geometric mean because of the logarithmic form of output.

From January to October 1974, the strip charts were analyzed by hand using the usual equal area method to produce hourly averages ending at a given hour. These hourly averages are also essentially geometric means because of the logarithmic form of output. Since there are four channels of output, 96 data points are produced for each day. Finally, three values of Angstrom exponent,  $\alpha$  (450, 550),  $\alpha$  (550, 700), and  $\alpha$  (700, 850) are calculated. In October 1974, the nephelometer was interfaced with the Mauna Loa data acquisition system, programmed to take one sample per second of the nephelometer output voltages, and to calculate hourly

means of the four light-scattering values. A comparison showed good agreement between manual strip chart analysis and computer analysis. Since all of the chart reduction was accomplished by the same person, it is believed that the data taken between January 1974 and October 1974 are probably as reliable as the subsequent computer-analyzed data. All data after October 1974 were taken directly from the computer output except for periods when the computer was down or otherwise occupied. During these periods, the data were filled in by manual chart reduction.

Mauna Loa data are presented in three ways: (1) hourly means of  $b_{sp}$  (550 nm) plotted as a time series for January 1974 through December 1976; (2) monthly means of  $b_{sp}$  (450, 550, 700, 850 nm) for each hour of the day for January 1974 through December 1976; (3) monthly means of  $b_{sp}$  (450, 550, 700, 850 nm) for 0100 to 0700 hours, plotted as a time series for January 1974 through December 1976. These data are presented in Appendices A-C, along with relative humidity and winds for angstrom exponent. The data are discussed below.



### 3.1 Data in Appendix A

Appendix A gives hourly means of  $b_{sp}$  (550 nm), plotted on a logarithmic scale, along with hourly means of relative humidity, wind direction, and speed. The angle of the wind arrow indicates the direction from which the wind is blowing; the length of the arrow indicates the speed. The length of the barb is equivalent to 5 knots or about  $2.5 \text{ m sec}^{-1}$  and may be used for scale. For example, the winds on February 18, 1974 (Fig. A1) are about 15 knots ( $7.5 \text{ m sec}^{-1}$ ) from the southeast.

The presentation in Appendix A shows the overwhelming influence of the local wind circulation. Often the classic wind regime (Mendonca, 1969) occurred with northerly daytime upslope winds bringing moist contaminated island air, and southerly nighttime down slope winds bringing dry background tropospheric air to the Observatory. A good example of this diurnal circulation may be seen clearly in the first two weeks of October 1974 (Fig. A5).

There appear to be three well-defined climatic regimes at Mauna Loa:

(1) The classical upslope-downslope circulation discussed above is usually present during the undisturbed tradewind regime in which the tradewind inversion (Mendonca and Iwaoka, 1969) may be penetrated by the thermally induced

daytime upslope wind flow. Nighttime lightscattering values are very low, of the order of  $10^{-7} \text{ m}^{-1}$ , and may be representative of the background tropospheric aerosol.

(2) Occasionally, the upslope-downslope circulation is overwhelmed by strong southeasterlies (e.g., December 1974, Fig. A6) apparently associated with a strong high pressure system in the vicinity of the islands. These periods bring the cleanest dry background conditions to Mauna Loa and often give light scattering values lower than  $10^{-7} \text{ m}^{-1}$ .

(3) Often periods of uncertain air mass origins appear (e.g., November 12-18, 1974, Fig. A6) in which low relative humidity and high light scattering values are associated with westerly winds, or January 22-30, 1976 (Fig. A13), in which the upslope-downslope winds are so light that the circulation probably does not have a chance to cleanse itself.

Of course, there are many exceptions to these three regimes; however, with a little practice it becomes easy to scan the time series and perceive the background level of about  $10^{-7} \text{ m}^{-1}$ . Ordinarily, this level is attained during periods of strong winds with a southerly component and often is approached during nighttime downslope wind conditions.



If we are to attempt to define the background tropospheric aerosol, we must first understand the local wind patterns and determine the air mass present at the site in order to identify the periods when the surface measurements at Mauna Loa are representative of the upper troposphere.

### 3.2 Data in Appendix B

Appendix B gives monthly means of  $b_{sp}$  (450, 550, 700, 850 nm) for all hours of the day. The upper portion of each graph shows  $\alpha$  (450, 550),  $\alpha$  (550, 700),  $\alpha$  (700, 850), the three most useful independent angstrom exponent values obtainable from 4-wavelength light scattering data. The angstrom exponent is calculated using the formula

$$\alpha(\lambda_1, \lambda_2) = \frac{\log b_{sp}(\lambda_1) - \log b_{sp}(\lambda_2)}{\log \lambda_1 - \log \lambda_2}$$

Since a larger value of angstrom exponent suggests relatively more small particles, most of the data in Figures B1-B7 suggest an absence of larger particles during nighttime clean conditions and a fairly uniform power-law size distribution (over the limited size range seen by the nephelometer) during the daytime hours. That is, the background aerosol appears to have a steepening size distribution for larger particle sizes. This is seen most clearly in the annual means of Figure B7

where  $\alpha_{34}$  is slightly larger during the night than during the day.

One obvious feature of Figures B1-B6 is that the diurnal variation in light scattering is greatest in fall and winter and minimal in the spring. However, the maximum value, occurring at about 1530 hr, is fairly uniform throughout the year whereas the early morning values show a pronounced annual cycle. The diurnal change amounts to about an order of magnitude and this must be caused by an increase in particle concentration rather than particle growth caused by the daytime increase in relative humidity. Pueschel et al. (1973) found that the effects of relative humidity at Mauna Loa could account for only about a 50% increase in light scattering. Furthermore, condensation nucleus counts nearly always increase markedly during a daytime upslope event (see, e.g., Pueschel and Mendonca, 1972).

Another important feature of Figures B1-B7 is that the cleanest time of day at Mauna Loa is during the hour just before sunrise. Although there is some variation throughout the year, the best time of day for sampling background air at Mauna Loa on a regular basis is the period from about 0100 to 0700 hr.



### 3.3 Data in Appendix C

Figure C1 gives monthly means of data plotted for all three years. The two most obvious features are the annual variation in light scattering with a maximum in about May, and the annual variation in angstrom exponent with a minimum at about the same time.

It is interesting that many atmospheric variables measured at Mauna Loa show an annual variation similar to that of light scattering. In particular, the atmospheric transmission, as derived from solar radiation data (Ellis and Pueschel, 1972), shows a pronounced minimum in the spring. Bodhaine and Pueschel (1974) suggested that these variations in transmission may very well be caused by variations in the tropospheric aerosol. They concluded that a variation in aerosol of only  $0.5 \mu\text{gm m}^{-3}$  at Mauna Loa could account for the seasonal change in transmission. The three-year monthly means given in Figure B-8 show a springtime maximum of  $b_{\text{sp}}(550 \text{ nm}) = 1.33 \times 10^{-6} \text{ m}^{-1}$  and a winter minimum of  $b_{\text{sp}}(550 \text{ nm}) = 1.33 \times 10^{-7} \text{ m}^{-1}$ . By using Charlson's relationship, these light scattering values may be converted to the equivalent mass concentrations  $0.5 \mu\text{gm m}^{-3}$  and  $0.05 \mu\text{gm m}^{-3}$ . This amounts to an annual variation of  $0.45 \mu\text{gm m}^{-3}$ , very near the value suggested by Bodhaine and Pueschel (1974). Therefore, it is seen that both the magnitude and phase of

atmospheric transmission variations at Mauna Loa are accounted for very well by variations in aerosol mass concentration.

### 4. SUMMARY

The data show that diurnal upslope-downslope wind circulation is present much of the time, giving background sampling conditions during the night and contaminated conditions during the day. Periods of strong southeasterlies give the cleanest sampling conditions. Occasional uncertain periods occur which may give either low or high scattering values and are difficult to interpret. Variations in atmospheric transmission measured at Mauna Loa are closely in phase with light scattering variations suggesting that under certain conditions the surface aerosol measurements are representative of the upper troposphere and that aerosols are primarily responsible for variations in the Mauna Loa atmospheric transmission measurements.

### 5. ACKNOWLEDGMENTS

I wish to thank Cris Maeda, Ed Lundin, and Bob Evans for their untiring assistance in data reduction.



## 6. REFERENCES

- Ahlquist, N. C., and R. J. Charlson, 1967. A new instrument for measuring the visual quality of air, J. Air Pollut. Control Assoc., 17, 467-469.
- Ahlquist, N. C., and R. J. Charlson, 1969. Measurement of the wavelength dependence of atmospheric extinction due to scatter, Atmos. Environ., 3, 551-564.
- Angstrom, A., 1929. On the atmospheric transmission of sun radiation and on dust in the air, Geogr. Ann., 11, 156.
- Beuttell, R. G., and A. W. Brewer, 1949. Instruments for the measurement of the visual range, J. Sci. Instrum., 26, 357-359.
- Bodhaine, B. A., and B. G. Mendonca, 1974. Preliminary four wavelength nephelometer measurements at Mauna Loa Observatory, Geophys. Res. Letters, 1, 119-122.
- Bodhaine, B. A., and R. F. Pueschel, 1974. Source of seasonal variations in solar radiation at Mauna Loa, J. Atmos. Sci., 31, 840-845.
- Butcher, S. S., and R. J. Charlson, 1972. An Introduction to Air Chemistry, Academic, New York.
- Charlson, R. J., 1972. Multiwavelength nephelometer measurements in Los Angeles smog aerosol, J. Colloid and Interface Sci., 39, 240-265.
- Charlson, R. J., H. Horvath, and R. F. Pueschel, 1967. The direct measurement of atmospheric light scattering coefficient of visibility and pollution, Atmos. Environ., 1, 469-478.
- Charlson, R. J., N. C. Ahlquist, H. Selvidge, and P. B. MacCready, Jr., 1969. Monitoring of atmospheric aerosol parameters with the integrating nephelometer, J. Air Pollut. Control Assoc., 19, 937-942.
- Crosby, P., and B. W. Koerber, 1963. Scattering of light in the lower atmosphere, J. Opt. Soc. Am. 53, 358-361.
- Ellis, H. T., and R. F. Pueschel, 1972. Solar radiation: absence of air pollution trends at Mauna Loa, Science, 172, 845-846.
- Junge, C. E., 1963. Air Chemistry and Radioactivity, Academic, New York.
- Mendonca, B. G., 1969. Local wind circulation on the slopes of Mauna Loa, J. Appl. Meteorol., 8, 533-541.
- Mendonca, B. G., and W. T. Iwaoka, 1969. The trade wind inversion at the slopes of Mauna Loa, Hawaii, J. Appl. Meteorol., 8, 213-219.
- Mie, G., 1908. A contribution to the optics of turbid media, especially colloidal metallic suspensions, Ann. Physik, 4(25), 377-445.
- Pueschel, R. F., and B. G. Mendonca, 1972. Sources of atmospheric particulate matter on Hawaii, Tellus, 24, 139-149.
- Pueschel, R. F., B. A. Bodhaine, and B. G. Mendonca, 1973. The proportion of volatile aerosols on the island of Hawaii, J. Appl. Meteorol., 12, 308-315.
- Rayleigh, Lord, 1871. On the light from the sky, its polarization and colour, Philos. Mag., 41, 107-120.
- Whitby, K. T., 1975. Modeling of atmospheric aerosol particle size distributions, Progress report on EPA grant No. R800971, Univ. of Minn., Minneapolis, Minnesota.
- Waggoner, A. P., N. C. Ahlquist, R. J. Charlson, 1976. Recent developments in nephelometers, In NASA CP 2004.



## Appendix A

Hourly means of 550 nm light scattering, relative humidity, and wind at 3-hour intervals for Mauna Loa Observatory.



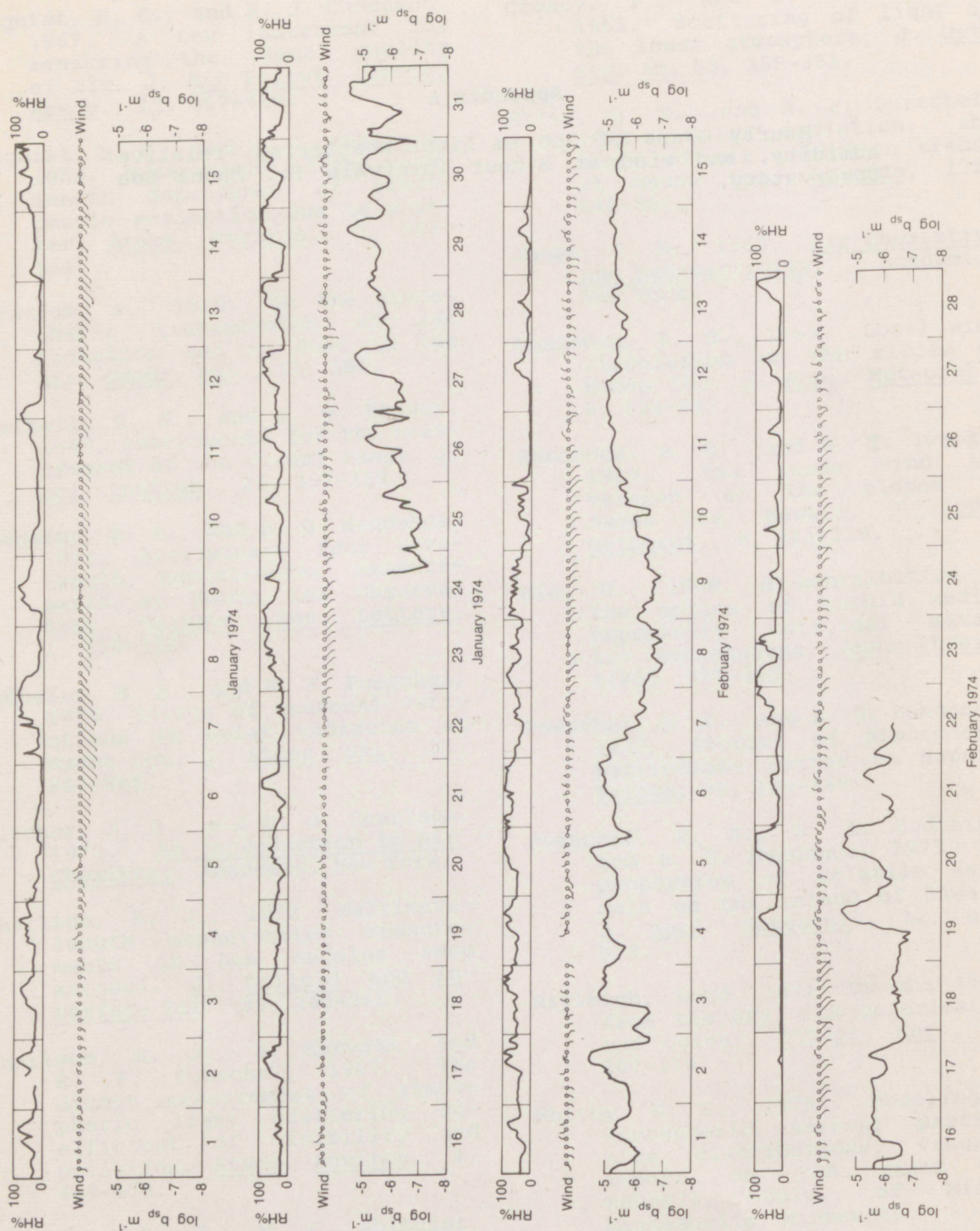


Figure A1. January-February 1974.



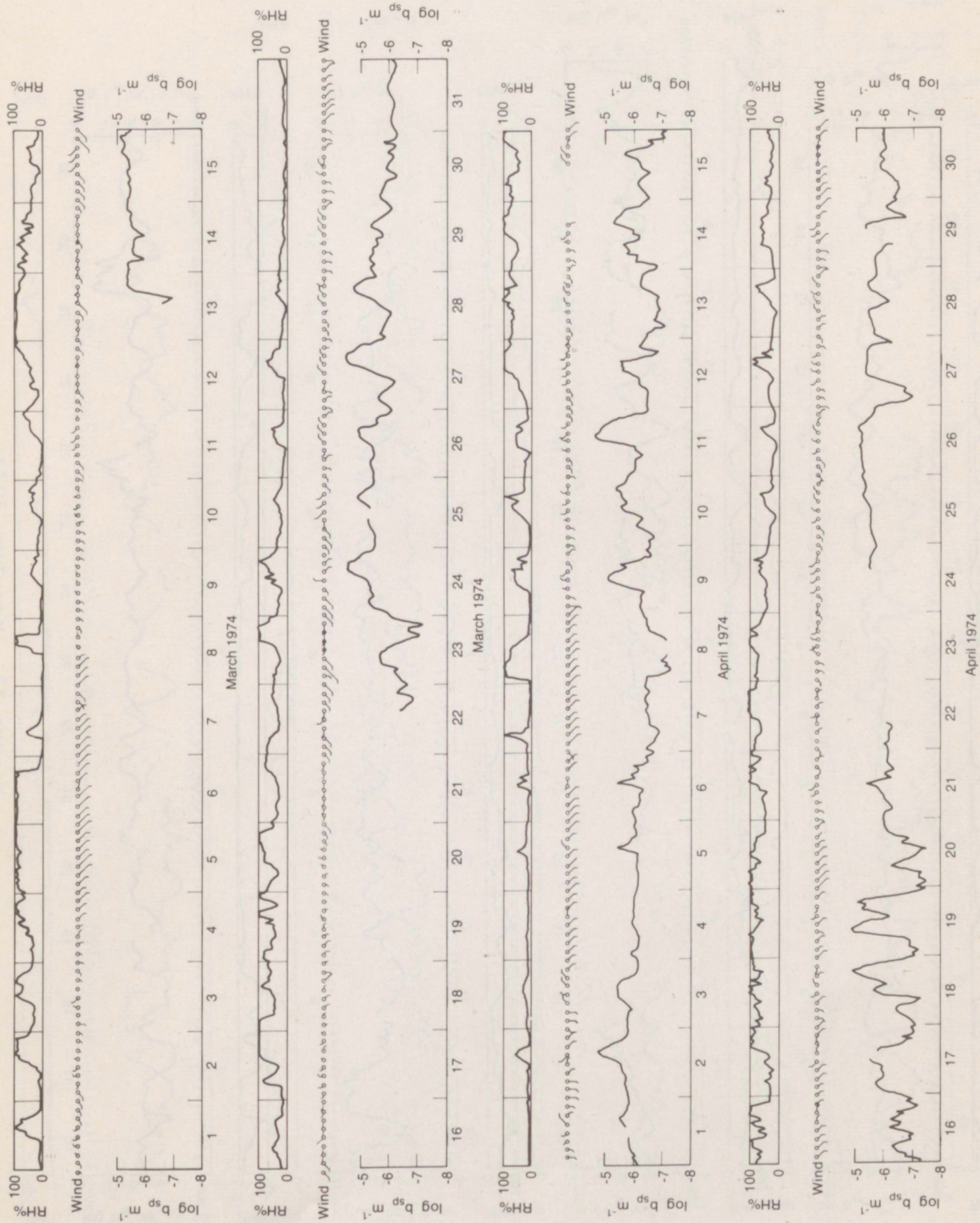


Figure A2. March-April 1974.



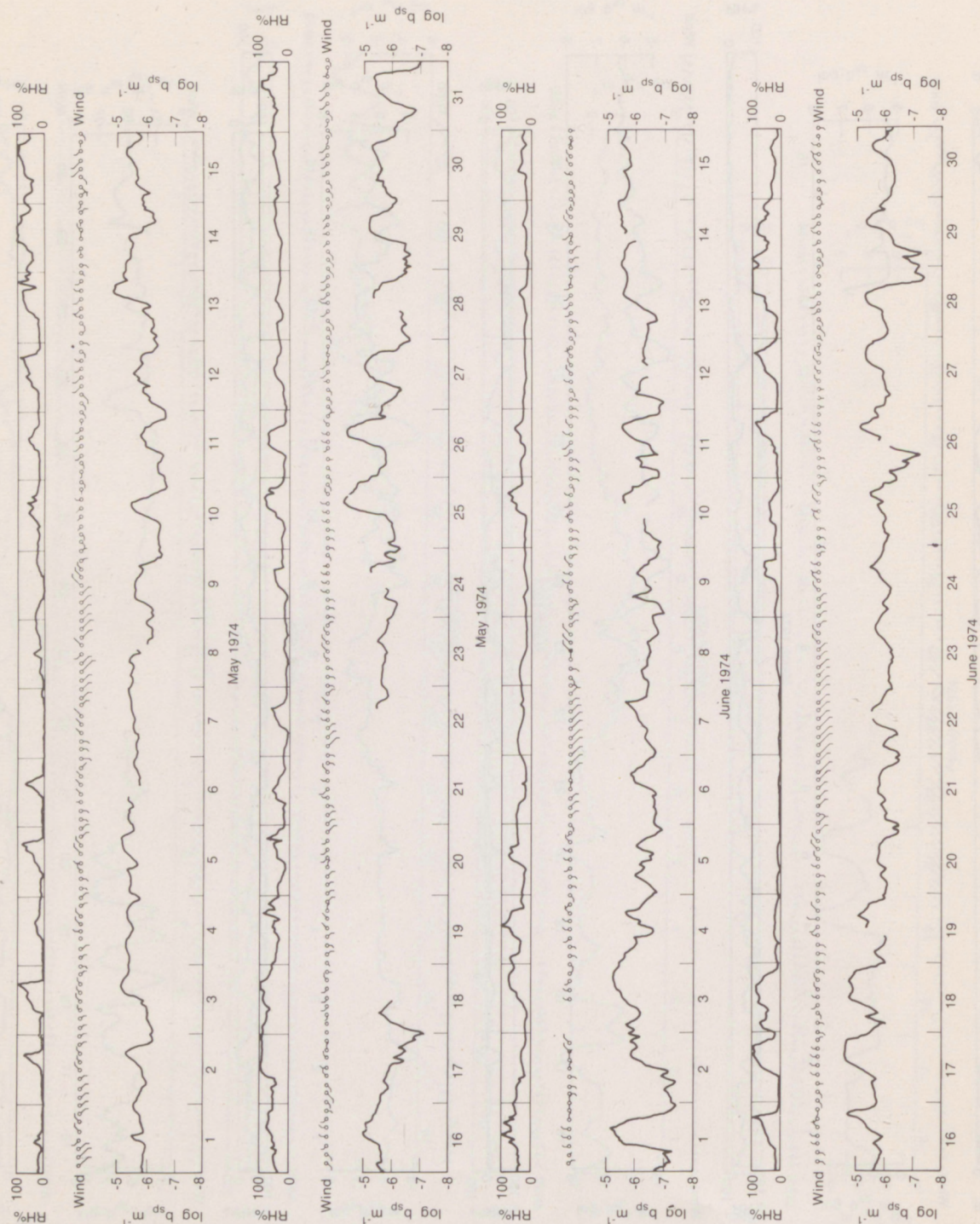


Figure A3. May-June 1974.



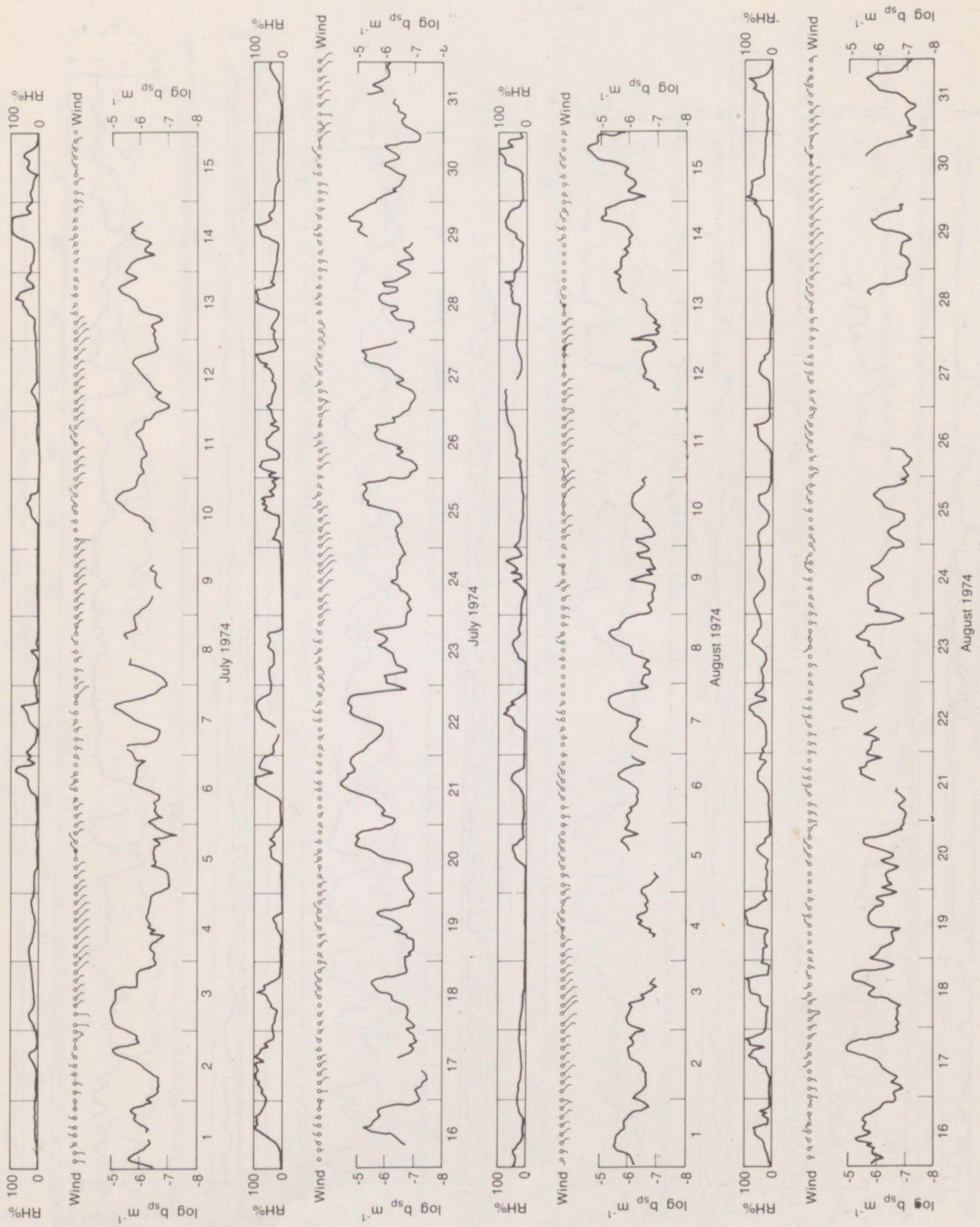


Figure A4. July-August 1974.



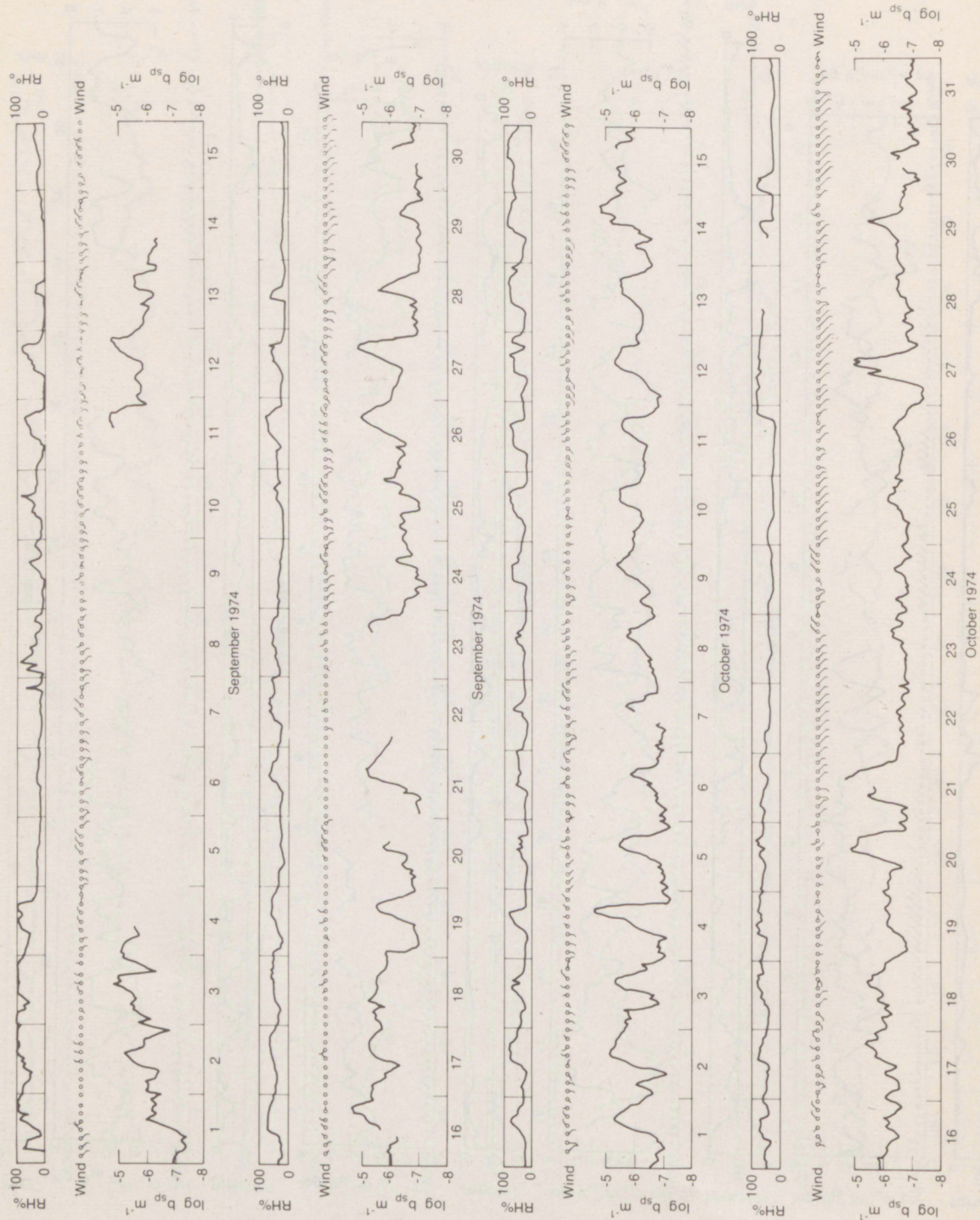


Figure A5. September-October 1974.



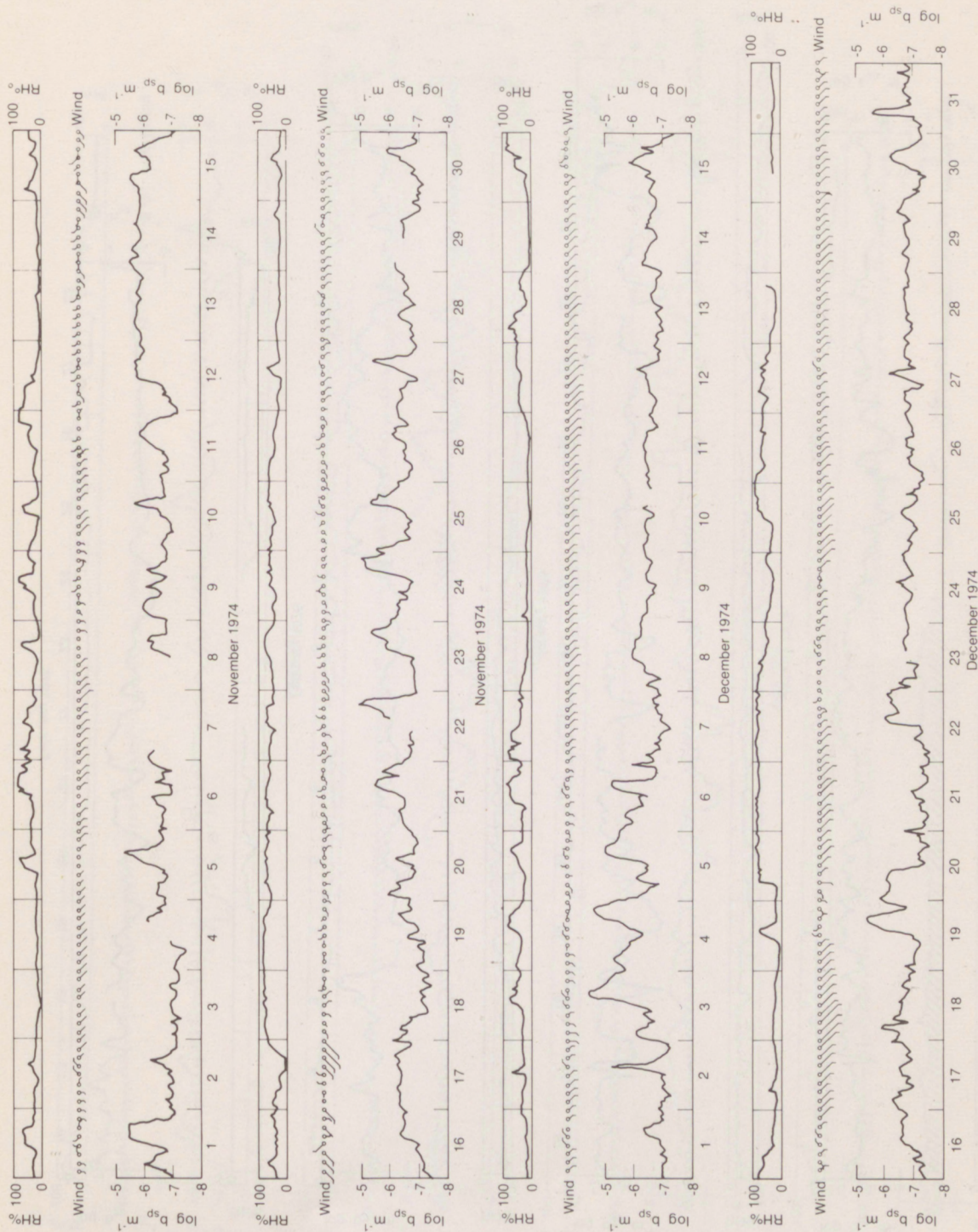


Figure A6. November-December 1974.



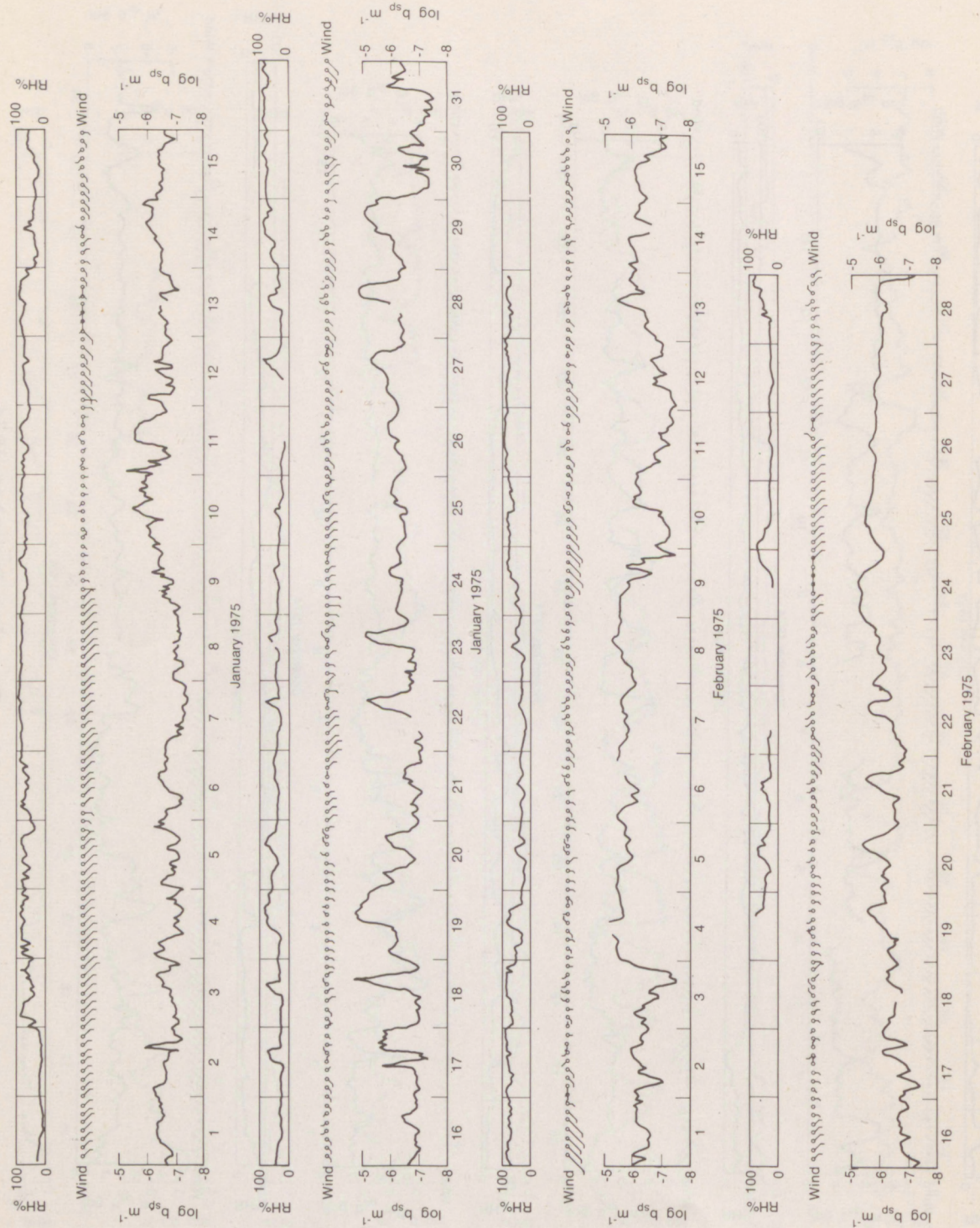


Figure A7. January-February 1975.



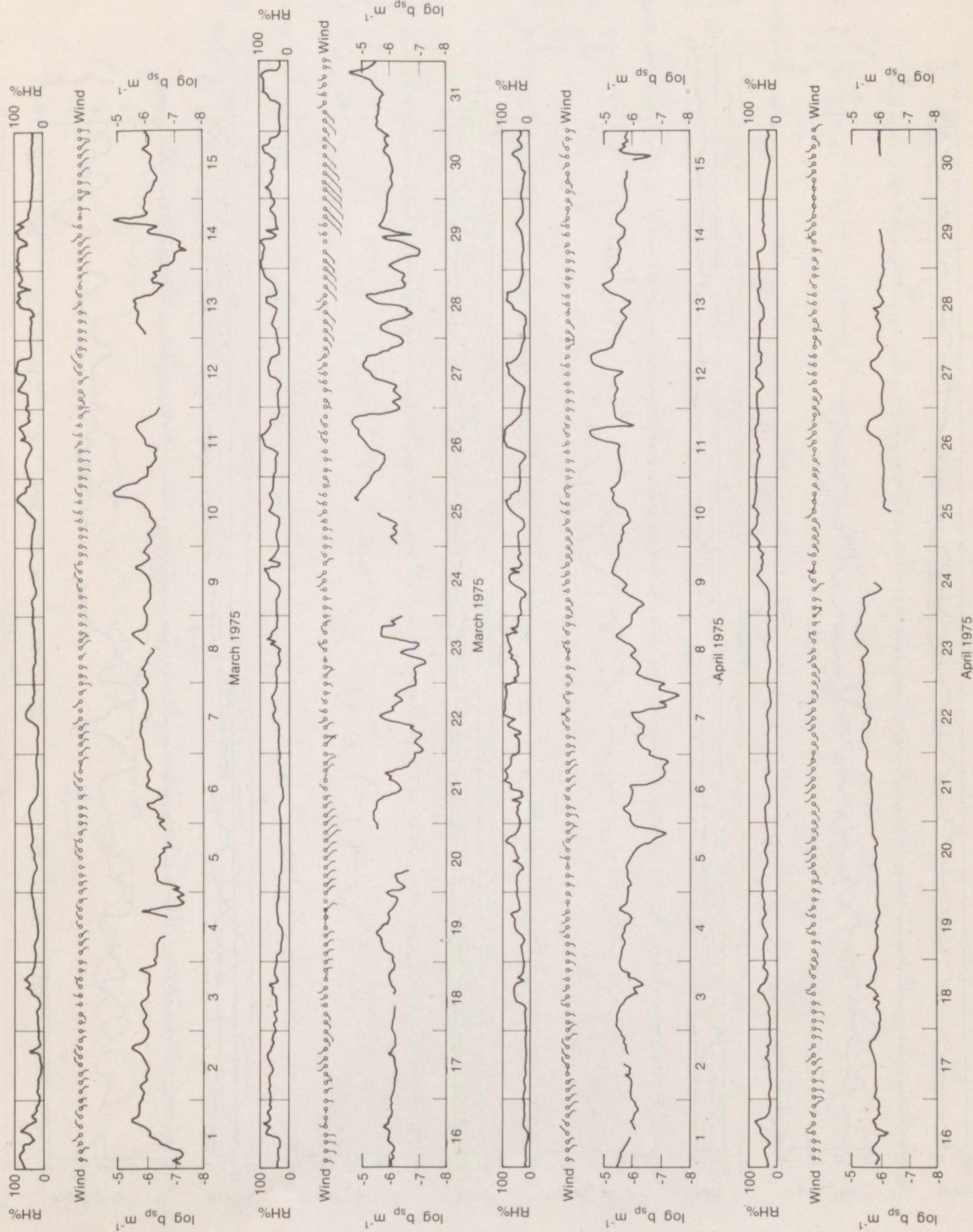


Figure A8. March-April 1975.



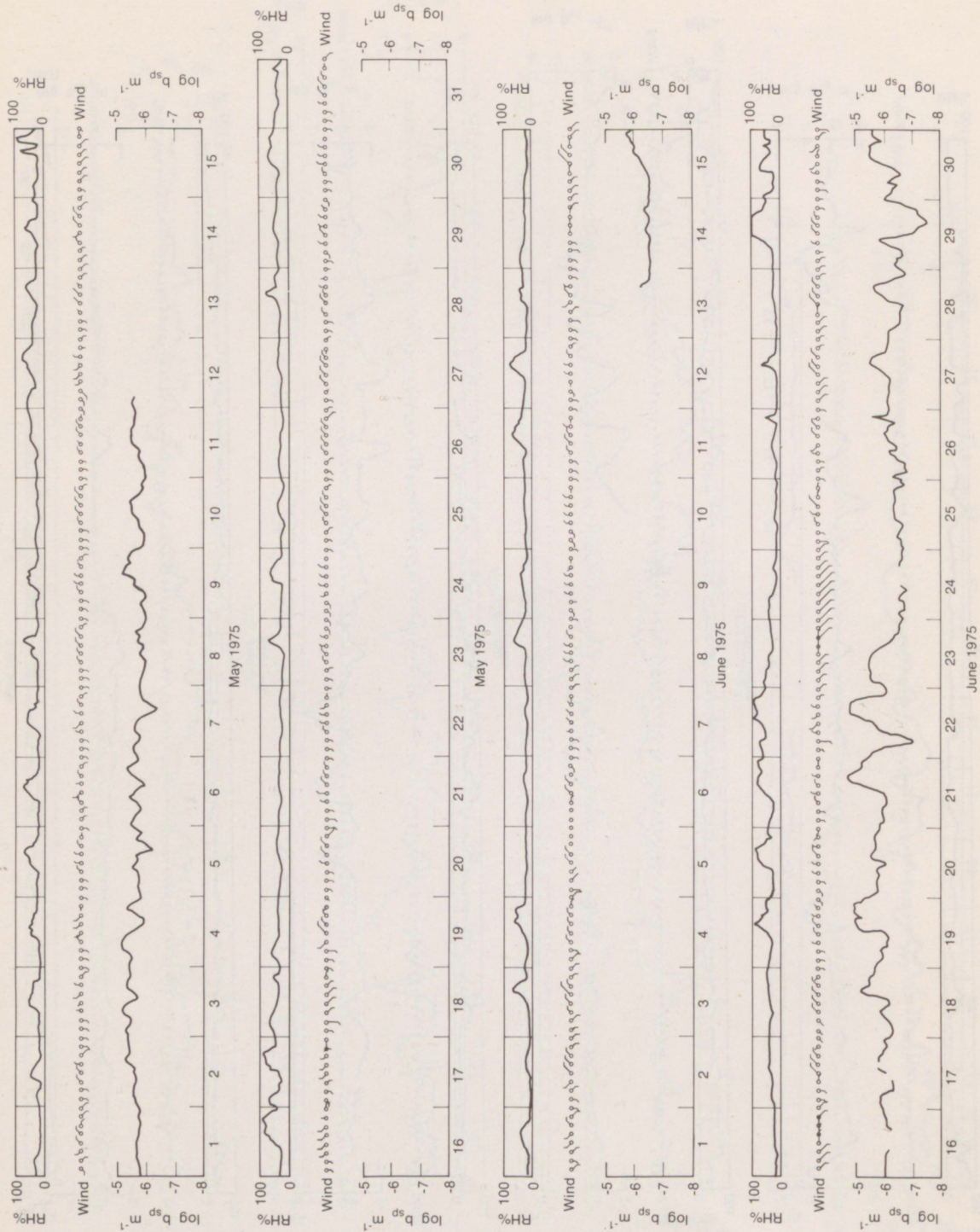


Figure A9. May-June 1975.



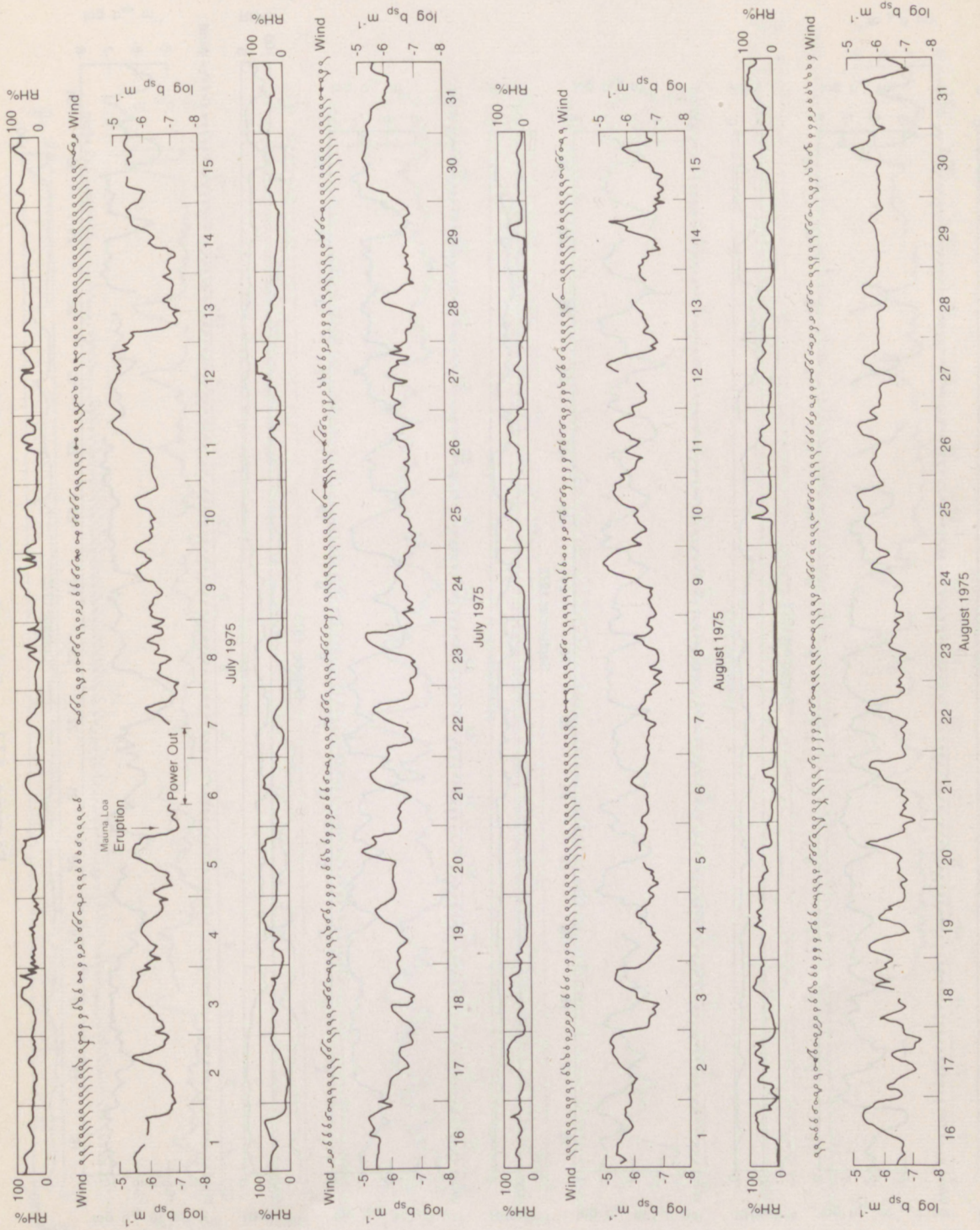


Figure A10. July-August 1975.



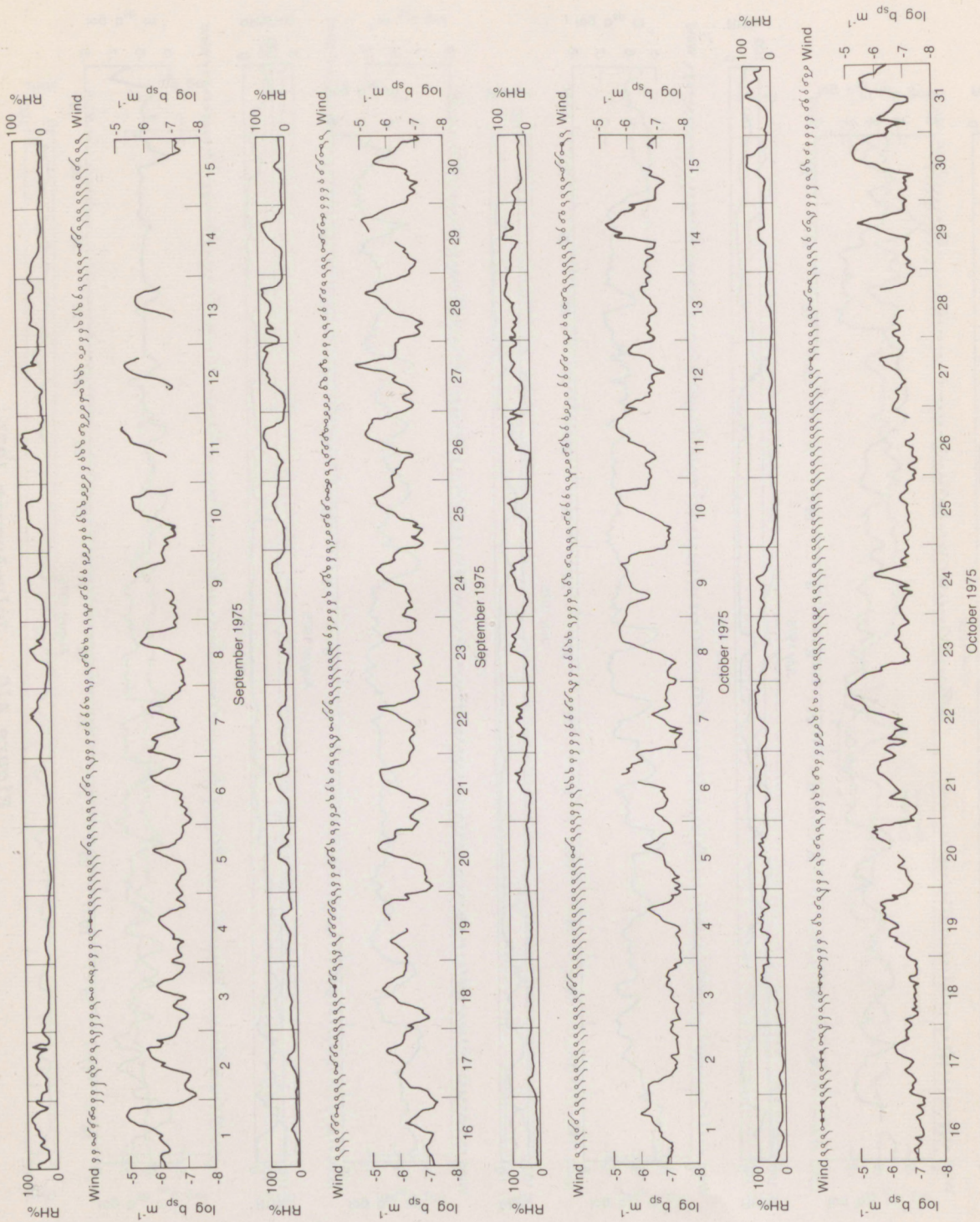


Figure A11. September-October 1975.



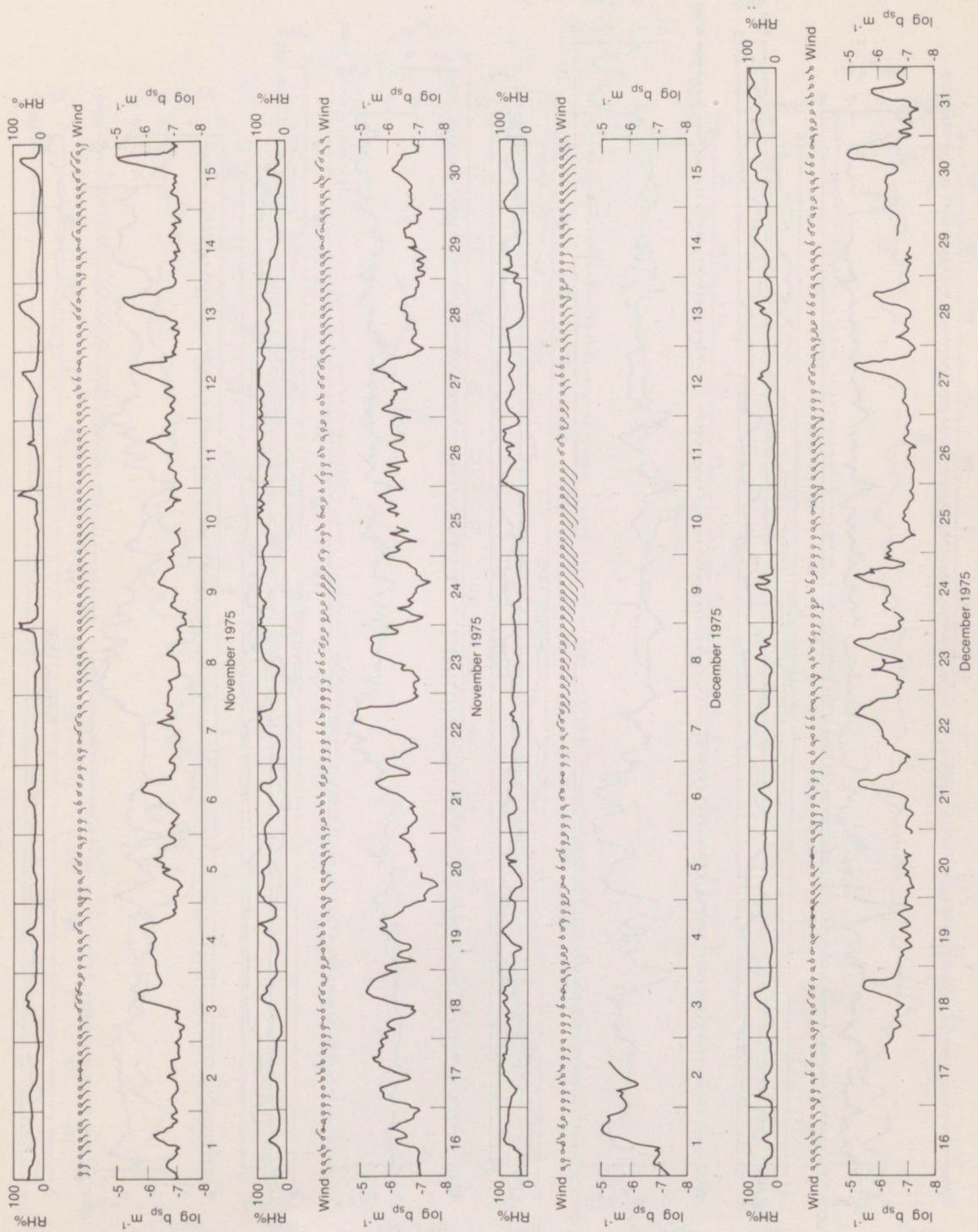


Figure A12. November-December 1975.



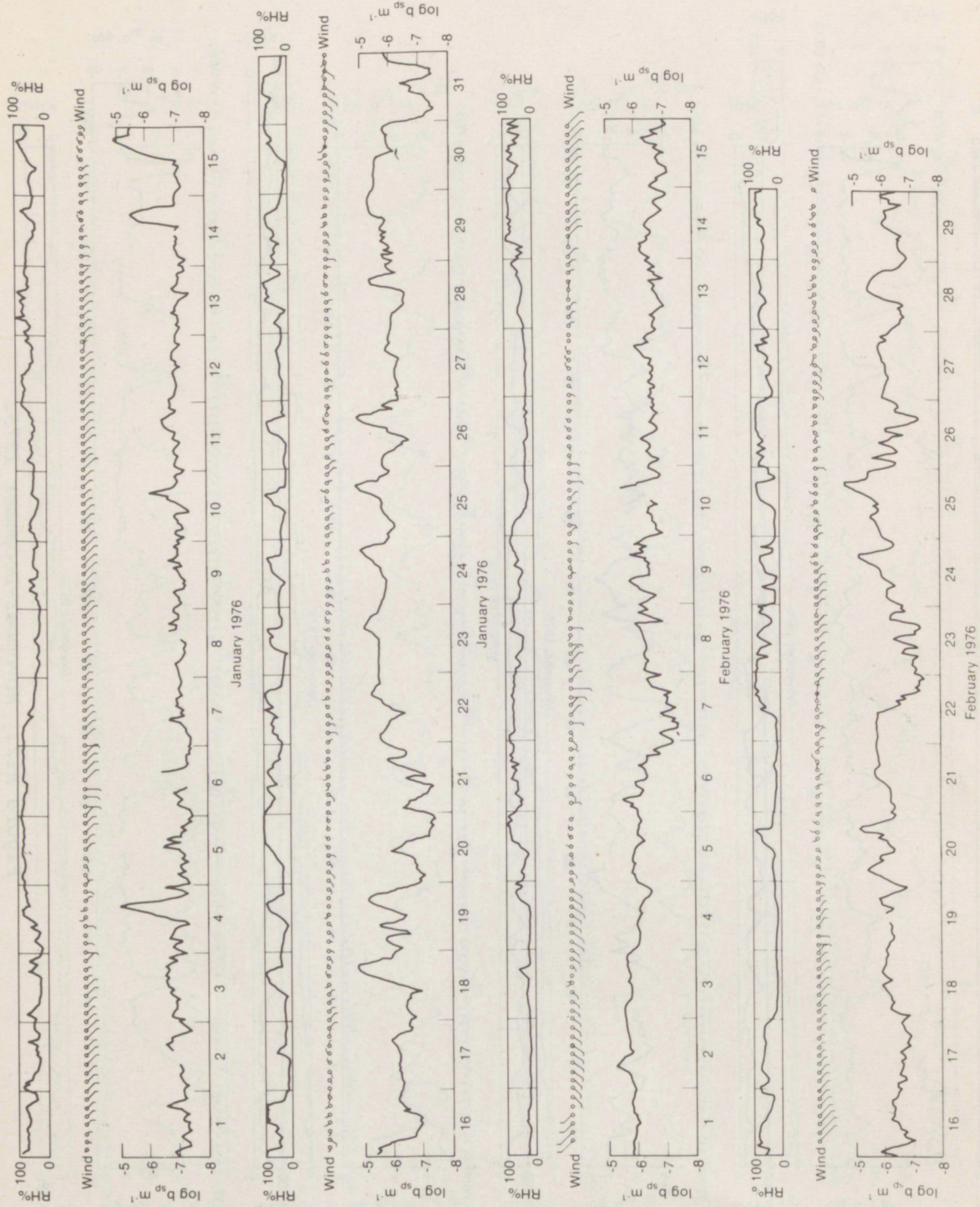


Figure A13. January-February 1976.



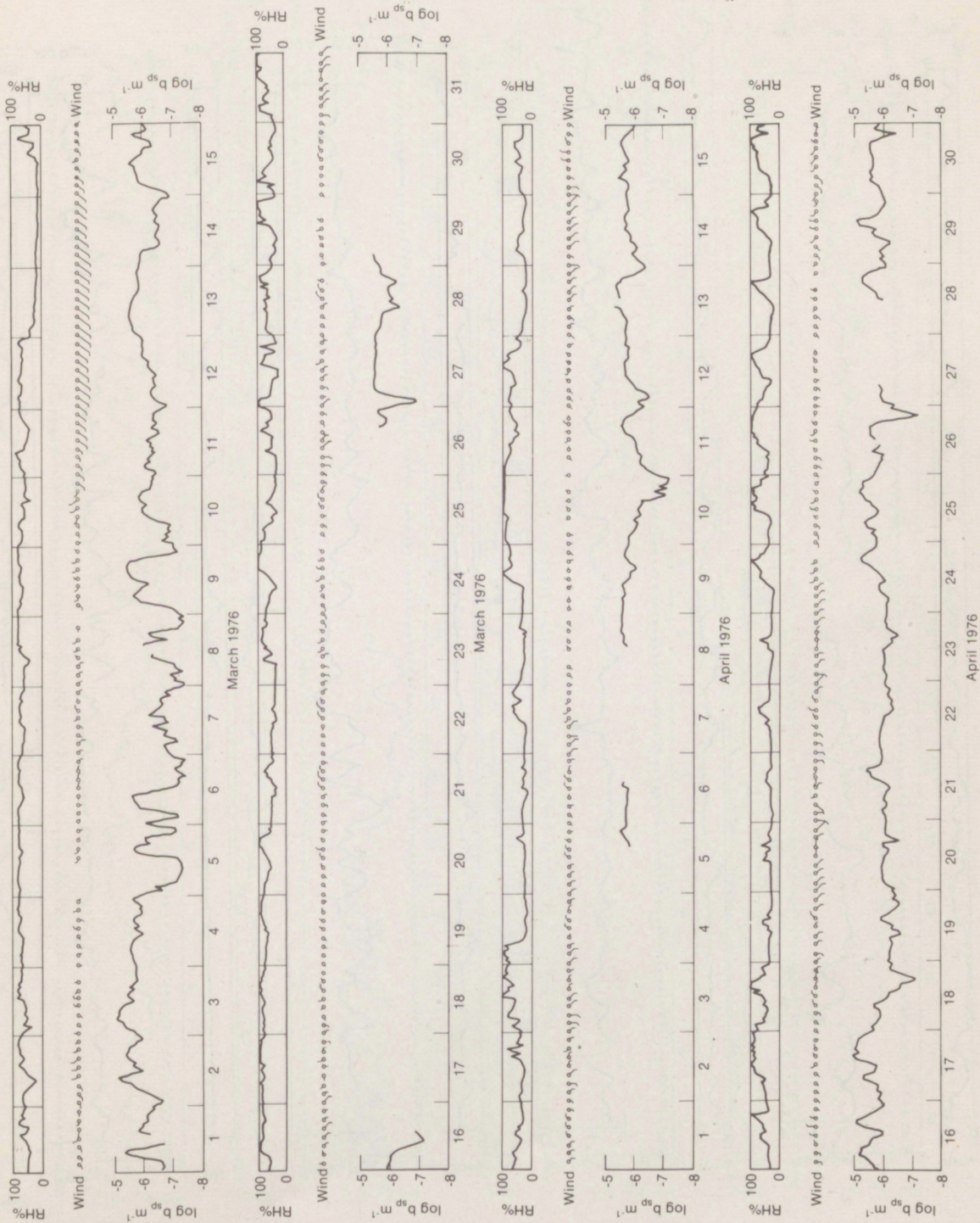


Figure A14. March-April 1976.



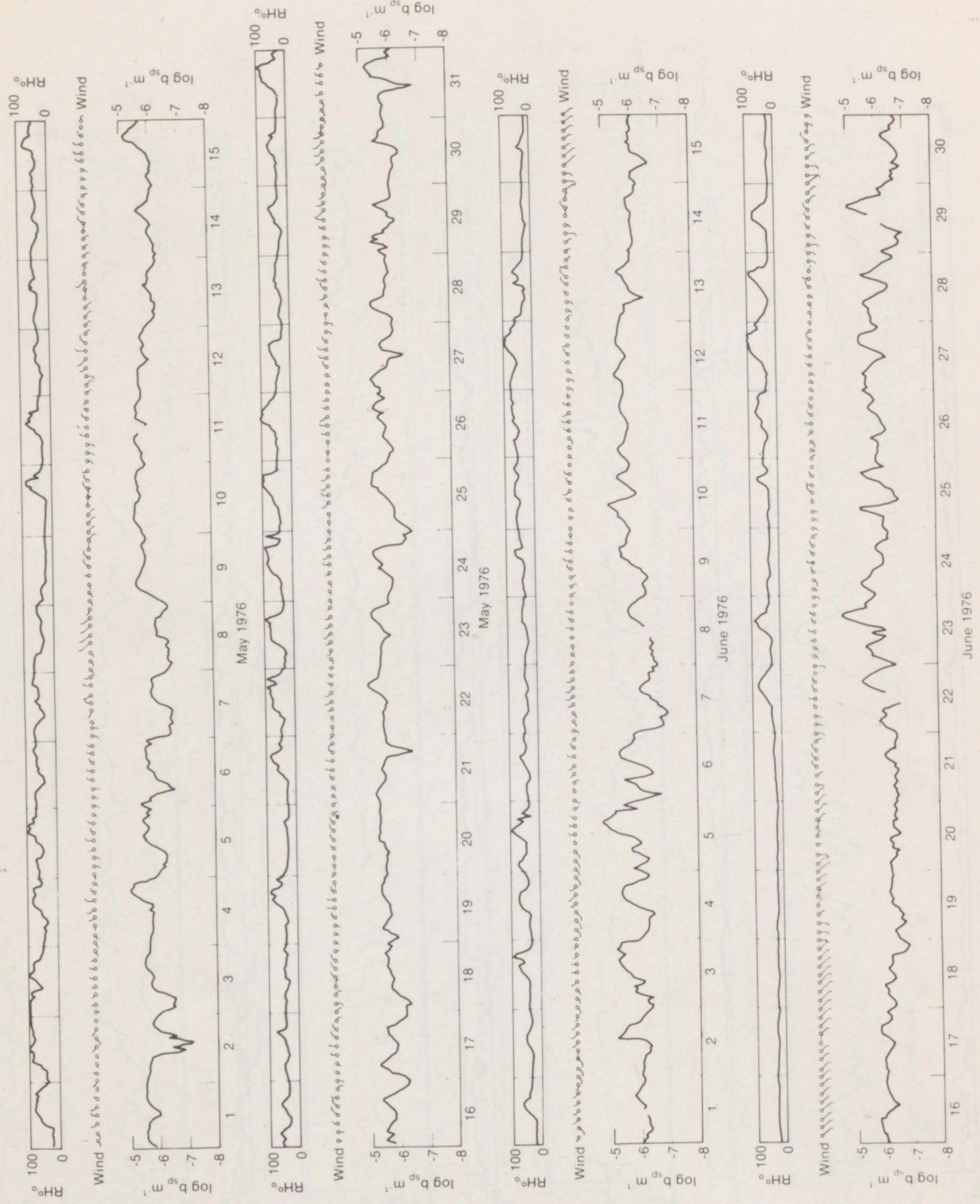


Figure A15. May-June 1976.



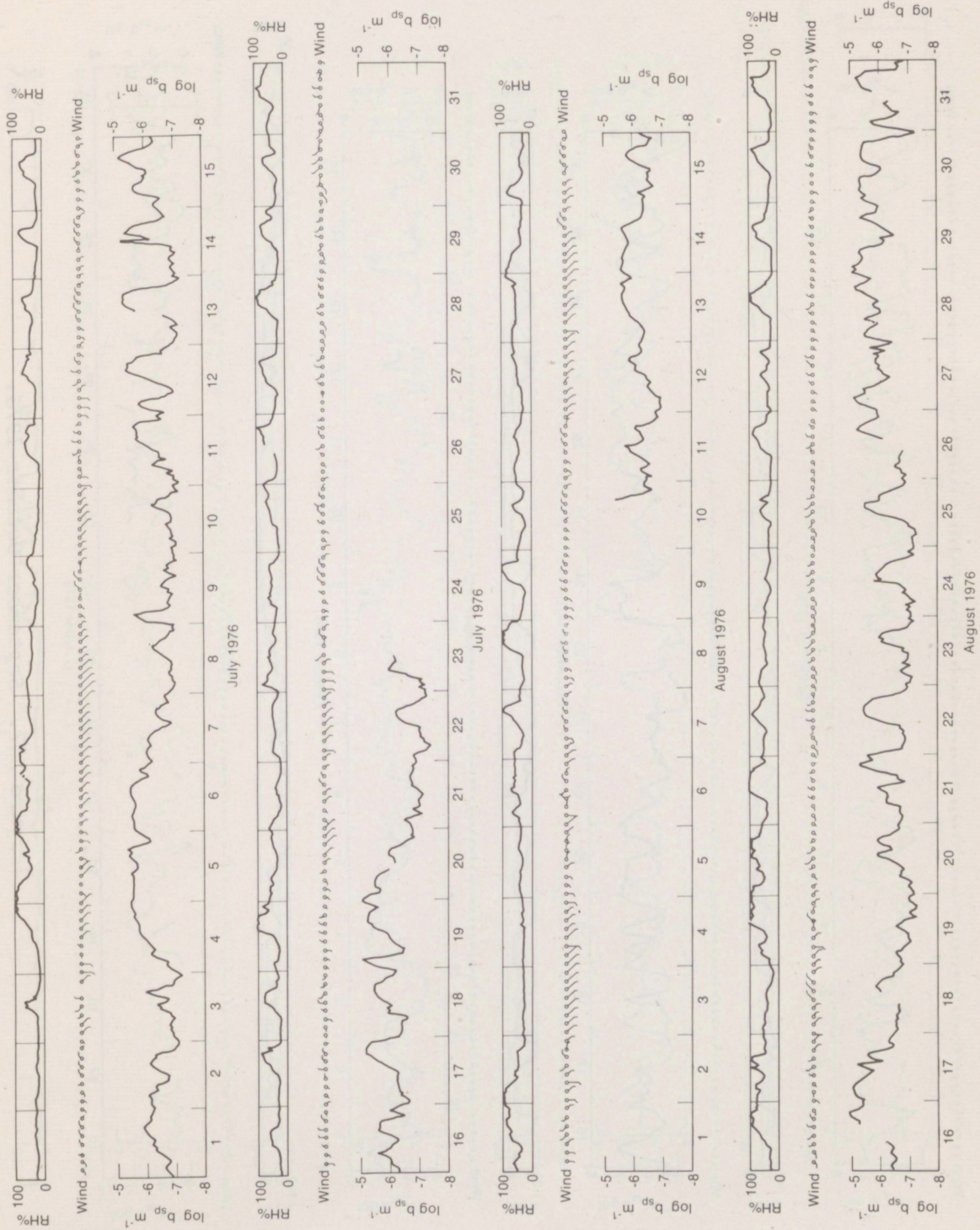


Figure A16. July-August 1976.



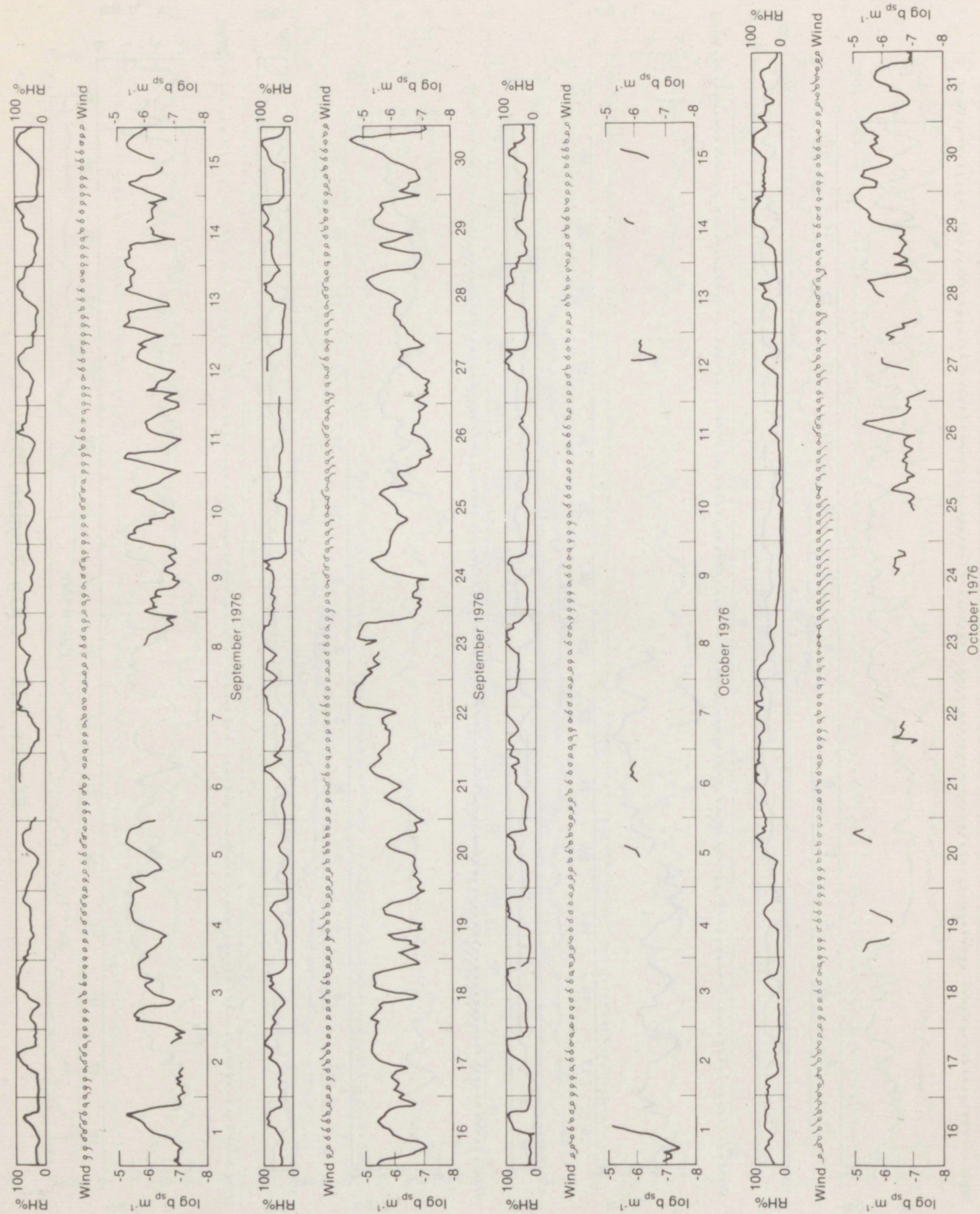


Figure A17. September-October 1976.



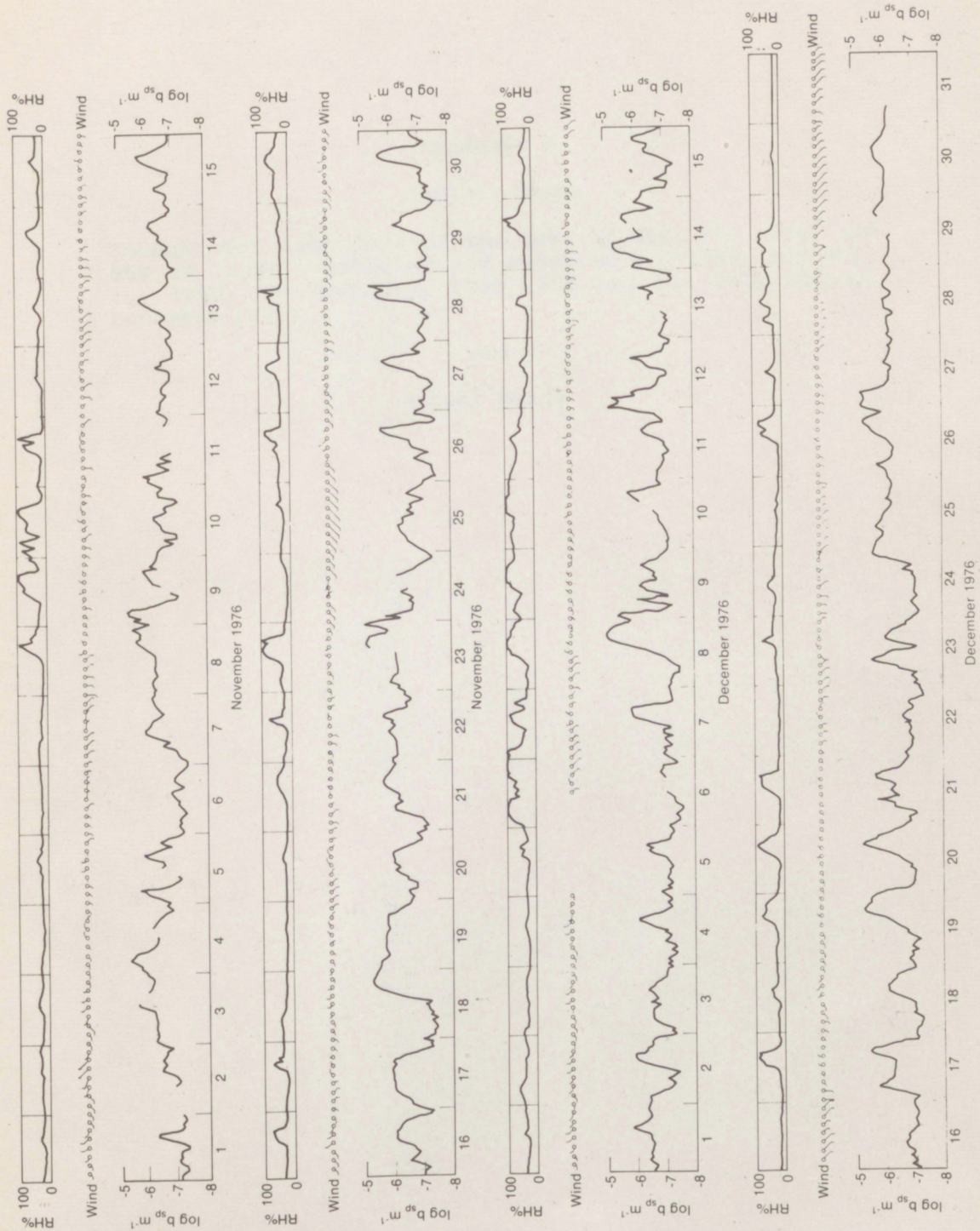


Figure A18. November-December 1976.







## Appendix B

### Monthly Means

[means, for each hour of the day, of 450, 550, 700, and 850 nm light scattering and angstrom  $\alpha_{12}$  (450, 500 nm),  $\alpha_{23}$  (550, 700 nm),  $\alpha_{34}$  (700, 850 nm) for July through December 1975]

and

### Annual Means



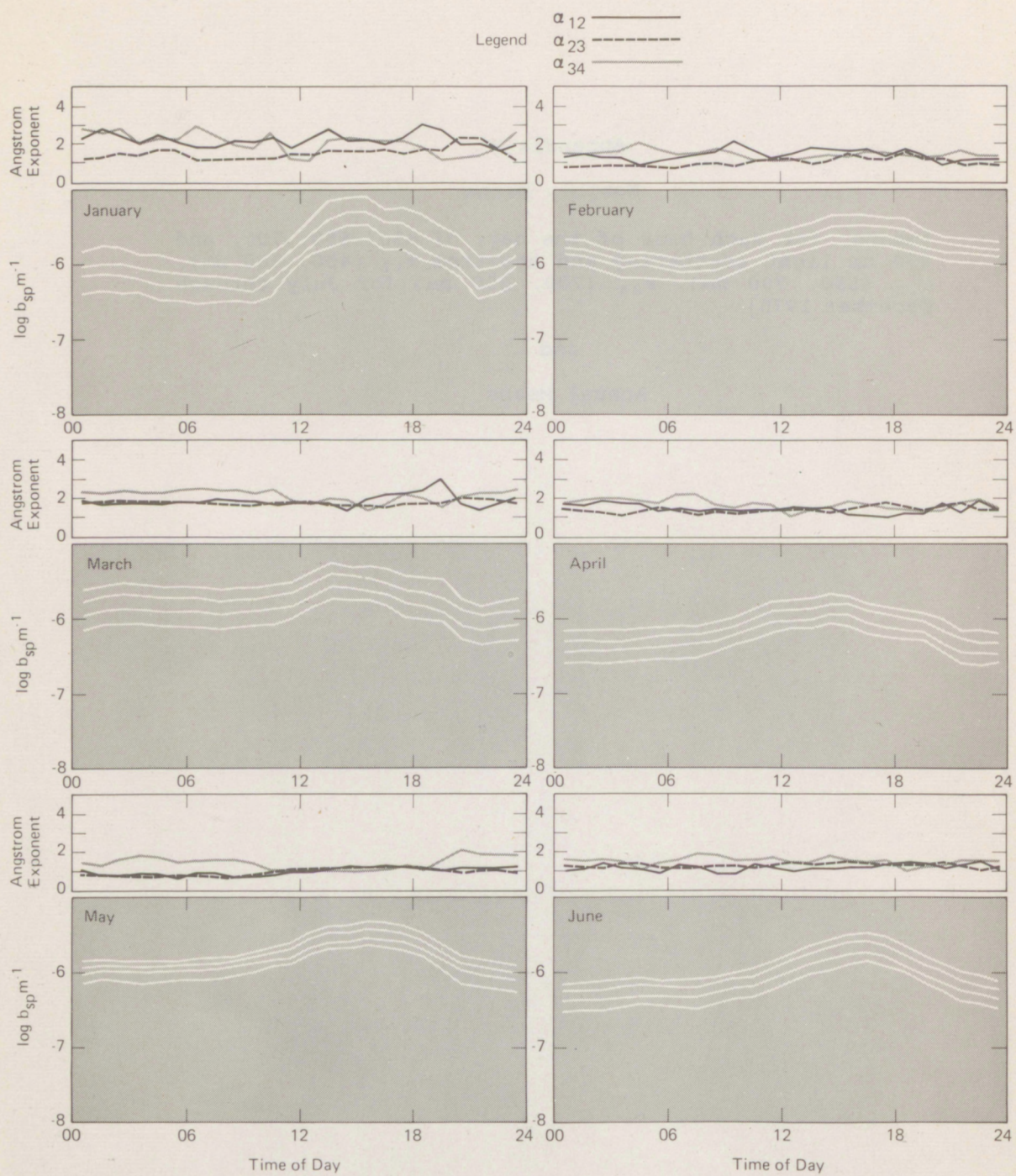


Figure B1. Monthly means for January-June 1974.



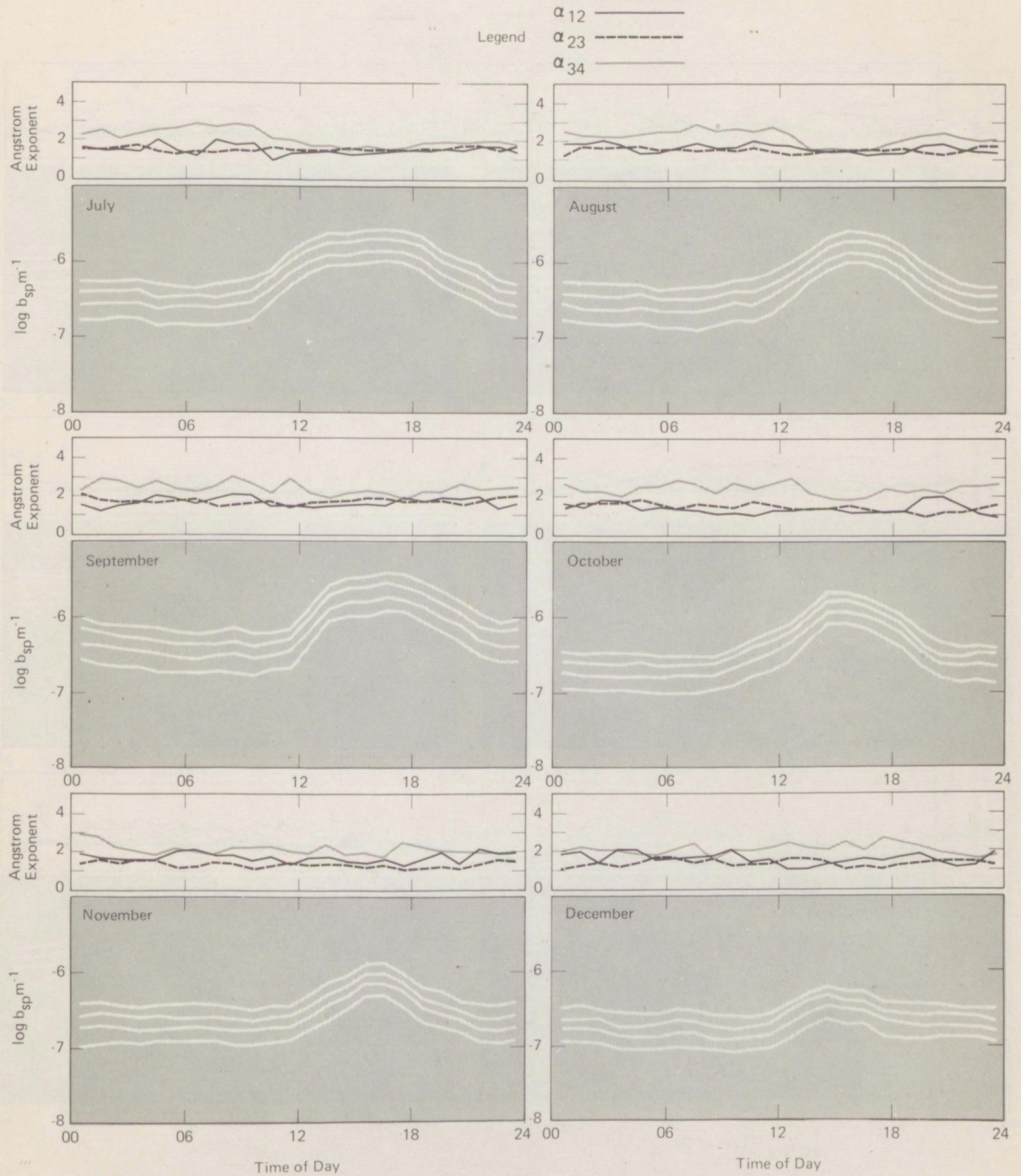


Figure B2. Monthly means for July-December 1974.



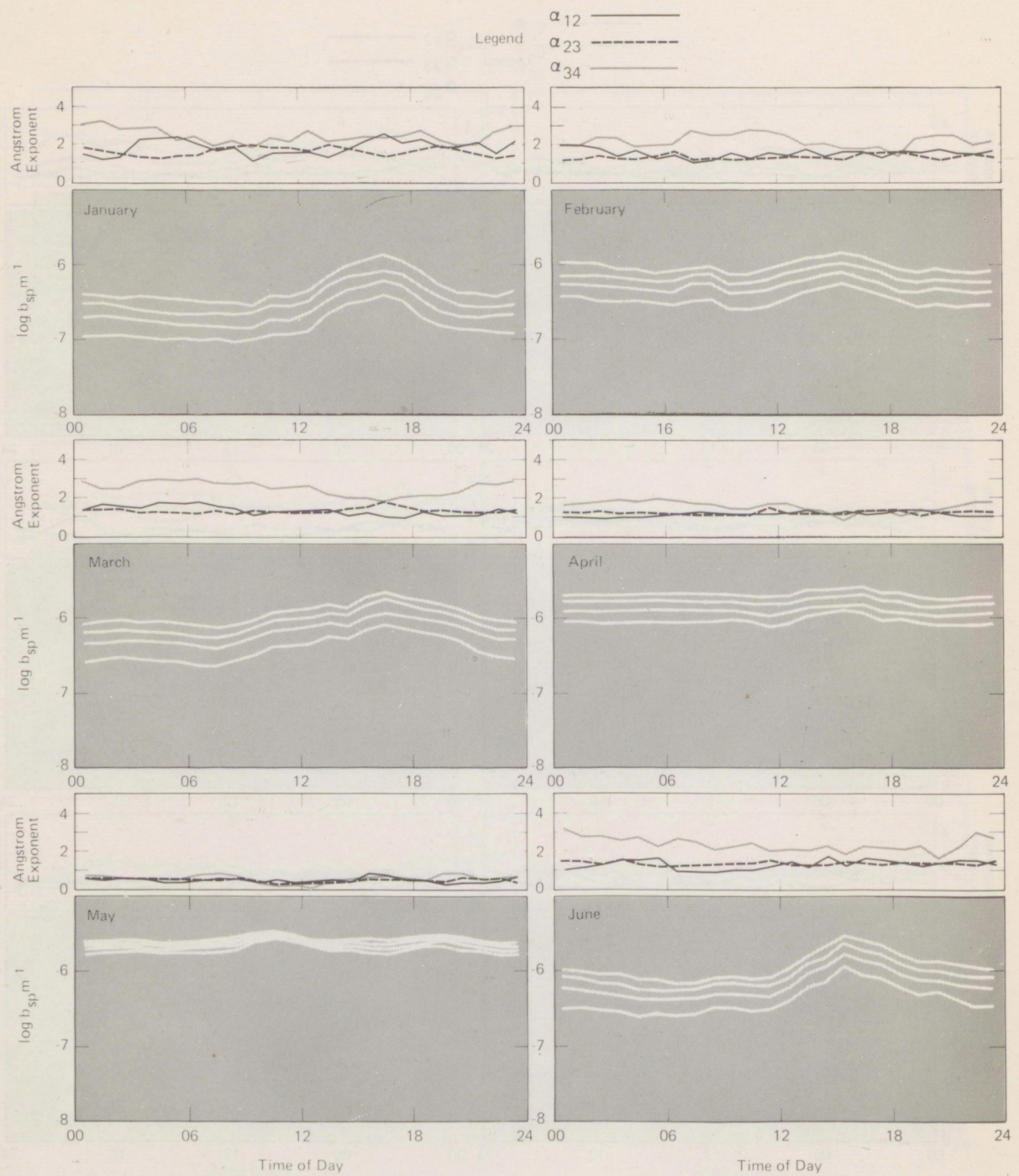


Figure B3. Monthly means for January-June 1975.



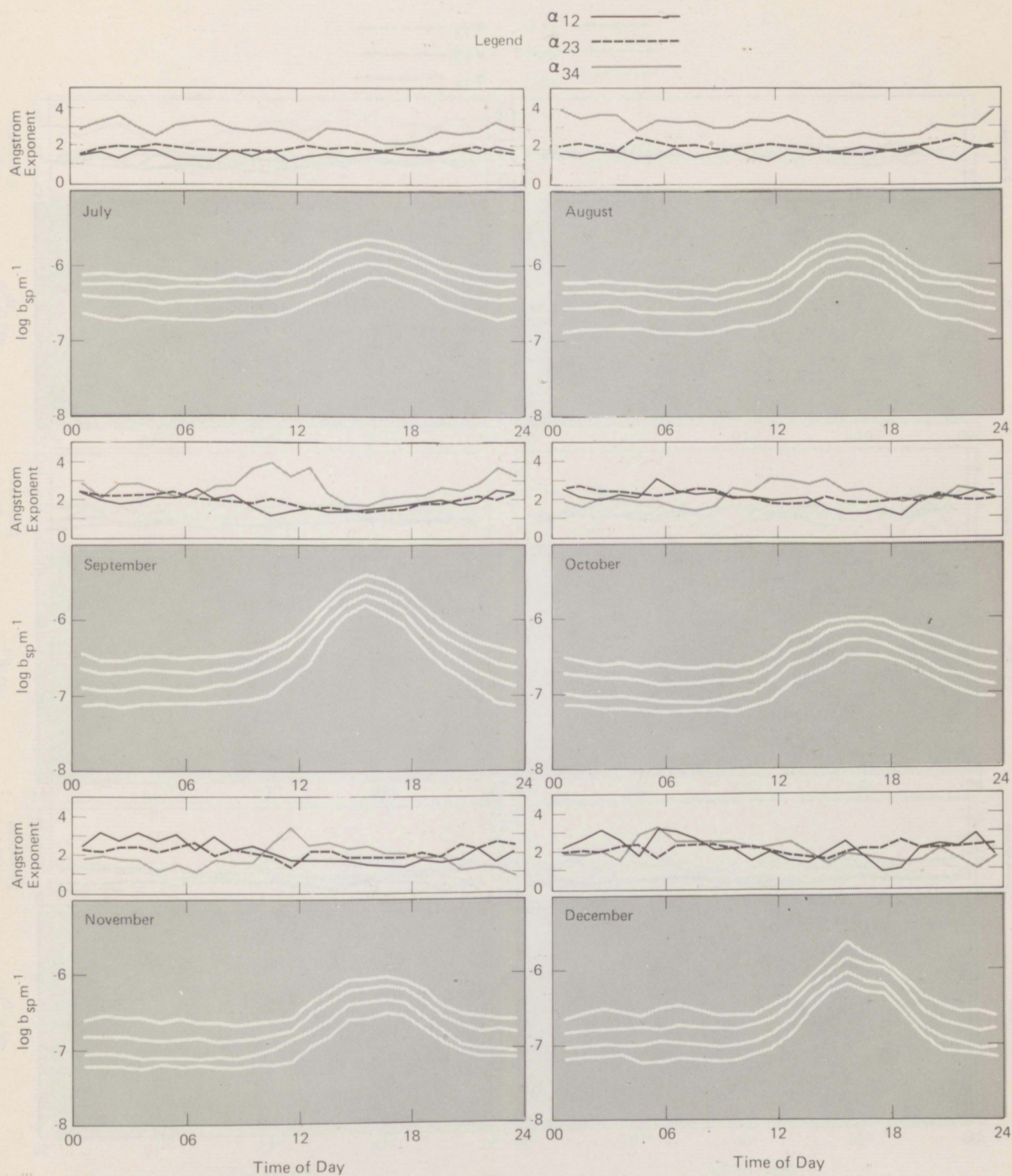


Figure B4. Monthly means for July-December 1975.



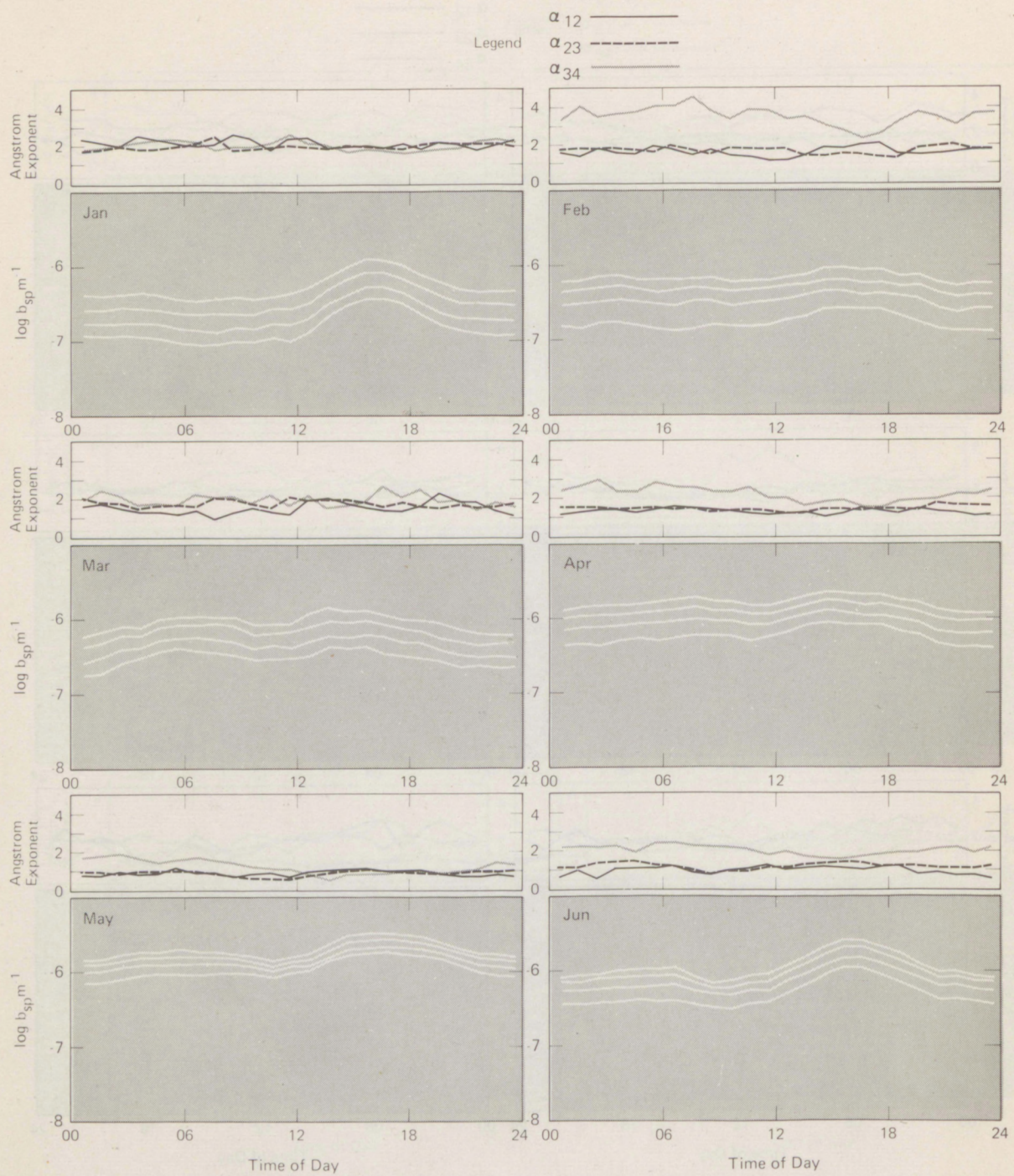


Figure B5. Monthly means for January-June 1976.



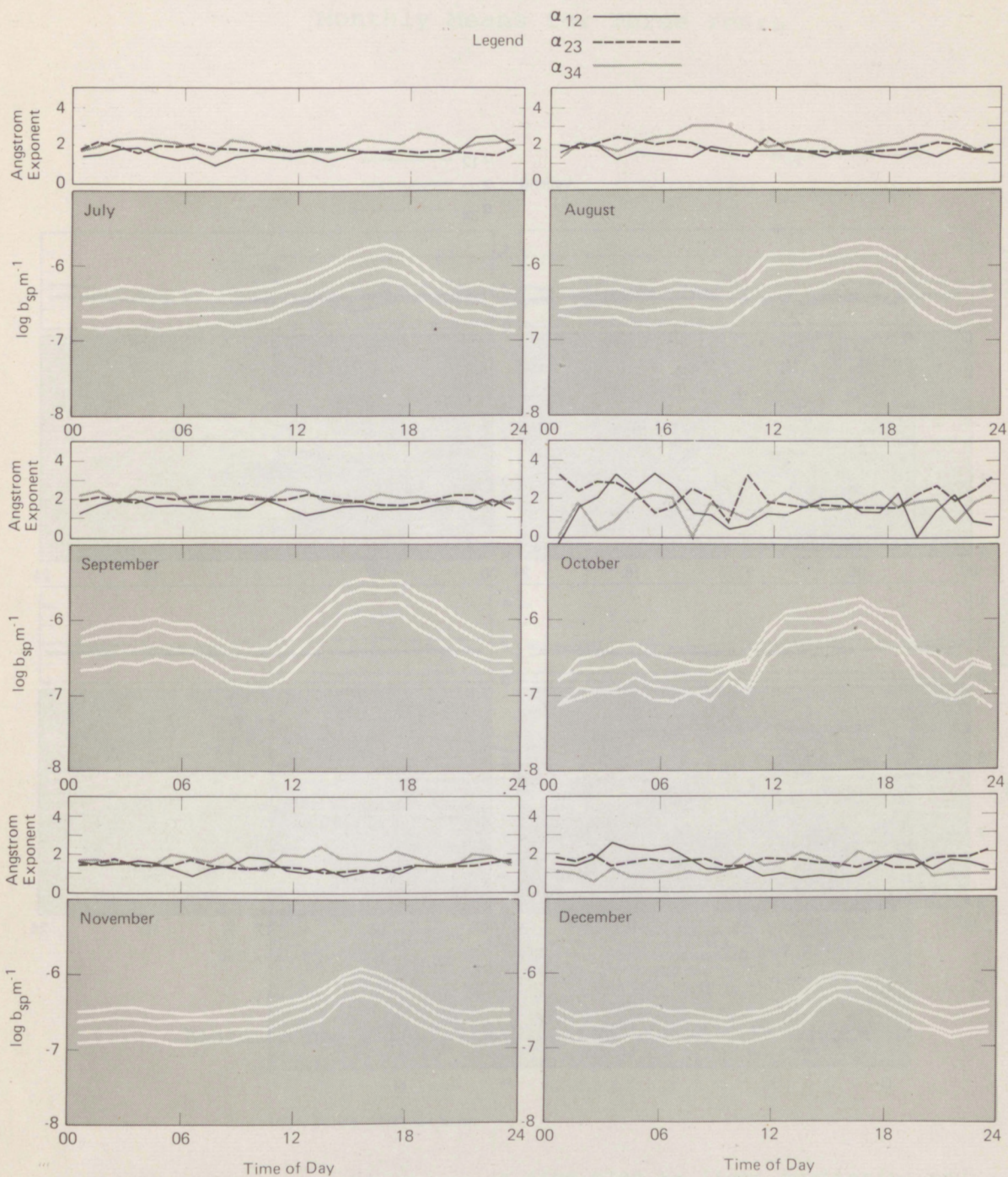


Figure B6. Monthly means for July-December 1976.



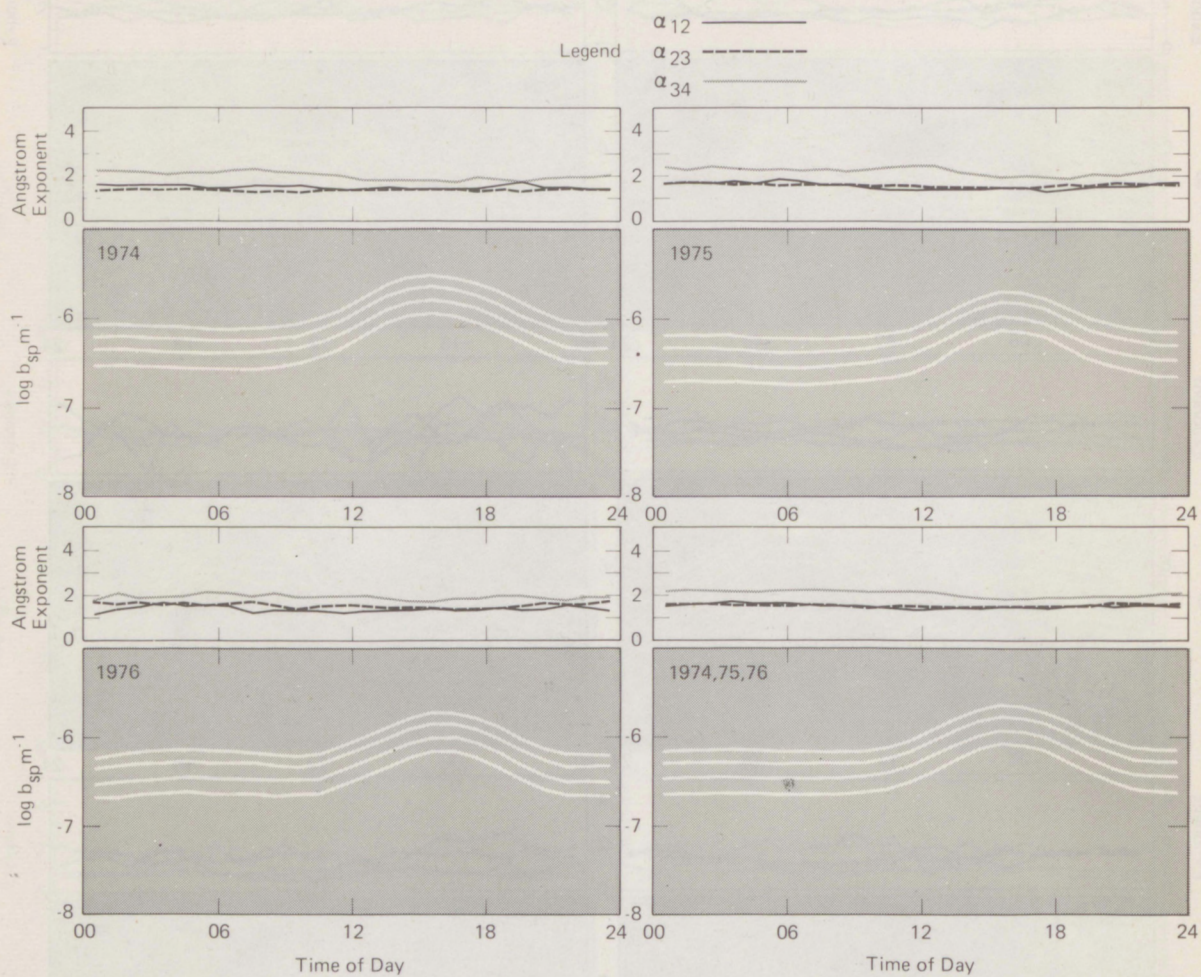


Figure B7. Annual means, individually and combined.



# Appendix C Monthly Means for Three Years

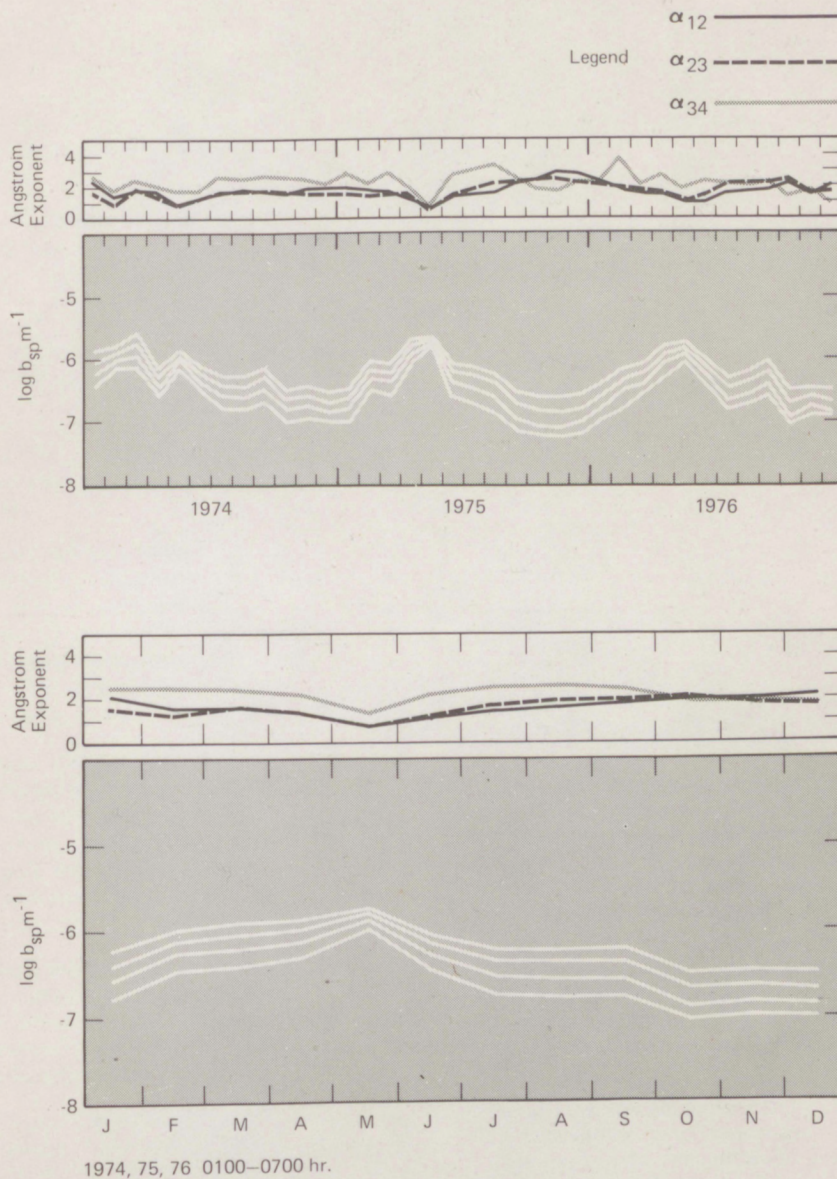


Figure C1. Monthly means of 0100-0700 hr light scattering and angstrom exponent for 1974, 1975, 1976, and for all three years combined.



# Environmental Research LABORATORIES

The mission of the Environmental Research Laboratories (ERL) is to conduct an integrated program of fundamental research, related technology development, and services to improve understanding and prediction of the geophysical environment comprising the oceans and inland waters, the lower and upper atmosphere, the space environment, and the Earth. The following participate in the ERL missions:

<b>MESA</b>	<i>Marine EcoSystems Analysis Program.</i> Plans, directs, and coordinates the regional projects of NOAA and other federal agencies to assess the effect of ocean dumping, municipal and industrial waste discharge, deep ocean mining, and similar activities on marine ecosystems.	<b>GLERL</b>	<i>Great Lakes Environmental Research Laboratory.</i> Studies hydrology, waves, currents, lake levels, biological and chemical processes, and lake-air interaction in the Great Lakes and their watersheds; forecasts lake ice conditions.
<b>OCSEA</b>	<i>Outer Continental Shelf Environmental Assessment Program Office.</i> Plans and directs research studies supporting the assessment of the primary environmental impact of energy development along the outer continental shelf of Alaska; coordinates related research activities of federal, state, and private institutions.	<b>GFDL</b>	<i>Geophysical Fluid Dynamics Laboratory.</i> Studies the dynamics of geophysical fluid systems (the atmosphere, the hydrosphere, and the cryosphere) through theoretical analysis and numerical simulation using powerful, high-speed digital computers.
<b>W/M</b>	<i>Weather Modification Program Office.</i> Plans and coordinates ERL weather modification projects for precipitation enhancement and severe storms mitigation.	<b>APCL</b>	<i>Atmospheric Physics and Chemistry Laboratory.</i> Studies cloud and precipitation physics, chemical and particulate composition of the atmosphere, atmospheric electricity, and atmospheric heat transfer, with focus on developing methods of beneficial weather modification.
<b>NHEML</b>	<i>National Hurricane and Experimental Meteorology Laboratory.</i> Develops techniques for more effective understanding and forecasting of tropical weather. Research areas include: hurricanes and tropical cumulus systems; experimental methods for their beneficial modification.	<b>NSSL</b>	<i>National Severe Storms Laboratory.</i> Studies severe-storm circulation and dynamics, and develops techniques to detect and predict tornadoes, thunderstorms, and squall lines.
<b>RFC</b>	<i>Research Facilities Center.</i> Provides aircraft and related instrumentation for environmental research programs. Maintains liaison with user and provides required operations or measurement tools, logged data, and related information for airborne or selected surface research programs.	<b>WPL</b>	<i>Wave Propagation Laboratory.</i> Studies the propagation of sound waves and electromagnetic waves at millimeter, infrared, and optical frequencies to develop new methods for remote measuring of the geophysical environment.
<b>AOML</b>	<i>Atlantic Oceanographic and Meteorological Laboratories.</i> Studies the physical, chemical, and geological characteristics and processes of the ocean waters, the sea floor, and the atmosphere above the ocean.	<b>ARL</b>	<i>Air Resources Laboratories.</i> Studies the diffusion, transport, and dissipation of atmospheric pollutants; develops methods of predicting and controlling atmospheric pollution; monitors the global physical environment to detect climatic change.
<b>PMEL</b>	<i>Pacific Marine Environmental Laboratory.</i> Monitors and predicts the physical and biological effects of man's activities on Pacific Coast estuarine, coastal, deep-ocean, and near-shore marine environments.	<b>AL</b>	<i>Aeronomy Laboratory.</i> Studies the physical and chemical processes of the stratosphere, ionosphere, and exosphere of the Earth and other planets, and their effect on high-altitude meteorological phenomena.
		<b>SEL</b>	<i>Space Environment Laboratory.</i> Studies solar-terrestrial physics (interplanetary, magnetospheric, and ionospheric); develops techniques for forecasting solar disturbances; provides real-time monitoring and forecasting of the space environment.

**U.S. DEPARTMENT OF COMMERCE**  
**National Oceanic and Atmospheric Administration**  
 BOULDER, COLORADO 80302